

Applied Geoinformatics II

Report

Detection of Clearance Spaces using ATKIS and Point Clouds from bDOM and LiDAR

Gabriel Danzl

Olaf Wysocki

10th February 2020

Index

1	Introduction	3
2	Previous works	4
3	Data and tools	4
3.1	ATKIS	4
3.2	bDOM	5
3.3	LiDAR	5
3.4	FME	6
4	Proposed workflow	7
4.1	Research questions	7
4.2	Project architecture	7
4.2.1	General outline of the project	7
4.2.2	Detailed workflow of the project	8
5	Study case areas	16
5.1	Bridge nr. 1 (urban area)	16
5.2	Bridge nr. 2 (rural area)	18
5.3	Bridge nr. 3 (rural area)	18
6	Results	19
6.1	Clearance space creation with bDOM, LiDAR and fusion of those – comparison	19
6.2	Extraction of point cloud subsets	21
6.3	Linear referencing system (LRS)	21
6.4	Automatic workflow to enrich ATKIS data	22
6.5	Point cloud as additional modelling aid	23
6.6	Mesh as additional modelling aid	24
6.7	Final results	24
6.7.1	Bridge nr. 1 (urban area)	24
6.7.2	Bridge nr. 2 (rural area)	25
6.7.3	Bridge nr. 3 (rural area)	27
7	Challenges	29
8	Summary and possible applications	31
9	Bibliography	32

1 Introduction

In a previous project, the Chair of Geoinformatics at Technical University Munich wanted to automatically determine based on ATKIS data, which routes farmers usually take to their agricultural fields. They compared their results with the true routes that the farmers told them. They noticed that the determined routes often are wrong because of underpasses where the farmers cannot drive through with bigger machines. ATKIS does not contain information neither on clearance space nor on clearance height. Thus, it was not possible to choose the correct routes.

The idea of this project is to enrich the two-dimensional ATKIS data with information on the clearance space. To fulfil this task, we use different three-dimensional data like point clouds.

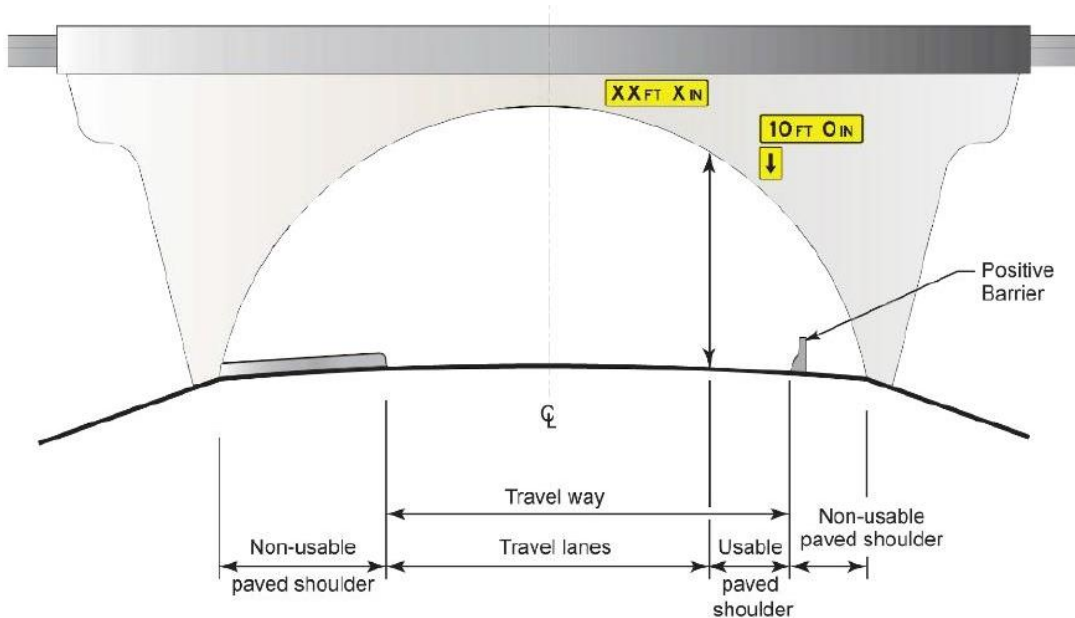


Figure 1, clearance space (Donaubauer, Nguyen, & Gackstetter, 2019)

The clearance space is defined by the curved profile shown in *Figure 1*. In reality, the profile is not always curved, it may also be shaped rectangularly. Often there are more objects in the scene beside the travel lanes. Pavements and barriers usually occur in urban scenes.

2 Previous works

Methods for automatic detection and depiction of clearance spaces and other overhead road assets using LiDAR data are introduced by companies (Consulting, 2020) as well as scientists (Gargoum, El-Basyouny, Gadowski, & Froese, 2017) (Liu, Chen, & Hasuer, 2012) (Puente, Akinci, González-Jorge, Díaz-Vilariño, & Arias, 2016). Most of the methods are based on LiDAR detests acquired by mobile scanners (Consulting, 2020) (Gargoum, El-Basyouny, Gadowski, & Froese, 2017), terrestrial static measurements (Liu, Chen, & Hasuer, 2012) or combination of terrestrial static scans, and close-range photogrammetry solutions (like Unmanned Aerial Vehicles (UAV) imagery) (Popescu, Täljsten, Blanksvärd, & Elfgren, 2019). Those works have demonstrated that it is possible to reconstruct 3D geometry of a bridge based on MLS (Mobile Laser Scanning) and TLS (Terrestrial Laser Scanning) and a combination of other close-range methods.

However, it is hard to observe research in the field of utilization of ALS (Aerial Laser Scanning) data to detect clearance spaces of bridges. Methods of 3D reconstruction of bridges based on aerial LiDAR data were focused on the reconstruction of top bridge surfaces (Ju, 2012) or were oriented to localize those objects (Sithole & Vosselman, 2006) (Wang, Peethambaran, & Chen, 2018). According to Ruisheng, Peethambaran and Chen distinguishing the ‘attached’ (connected to the bare earth, e.g. bridges) objects from the bare earth is a challenge work, therefore an accurate reconstruction of such objects become a hard problem (Wang, Peethambaran, & Chen, 2018). Moreover, in works dealing with the reconstruction of anthropogenic objects passages underneath bridges and multi-level road crossings are often discarded (Vosselman, Elberink, Post, Stoter, & Xiong, 2015) (Cheng, et al., 2015).

Nevertheless, researchers see potential in the combination of vector topographic data and ALS to reconstruct bridge objects (Wang, Peethambaran, & Chen, 2018). Elberink and Vosselman proposed a solution to connect road surfaces lying underneath bridges fusing 2D cadastre information with ALS data and estimating missing underneath bridge passage (Elberink & Vosselman, 2006). However, they acknowledge that the solution is highly dependent on accurate cadastre information (Elberink & Vosselman, 2006).

In our work, we would like to introduce a new approach and analyse different sources of aerially acquired spatial information in the field of bridge geometry reconstruction. We think that our results will introduce new insights to the reconstruction of overhead assets and allow to further develop this field of studies.

3 Data and tools

3.1 ATKIS

ATKIS is an abbreviation for the German designation “*Amtliches Topographisch Kartographisches Informationssystem*”. It is a collection of all the topographic objects like roads, rivers or railway lines. The data format we use is shapefile. Besides the geometric information, the data also contains additional attributes like the road hierarchy in the case of roads for example. One attribute we are interested in is HDU_X for roads and railway lines (Fiutak, Marx, Willkomm, & Donaubauer, 2018). A value of one depicts that this segment is above another segment. This may be a hint to detect bridges. The red lines in *Figure 2* show the railway axis for this area stored in ATKIS.



Figure 2, ATKIS data with OpenStreetMap

3.2 bDOM

This term means “bildbasiertes Digitales Oberflächenmodell”. It is a high-resolution digital surface model that was created using dense image matching. The format of this bDOM is a three-dimensional point cloud. The benefit is that each point also contains colour information. The points have high relative accuracy. An example point cloud is shown in *Figure 3*.



Figure 3, example of bDOM dataset

3.3 LiDAR

LiDAR is the abbreviation for “light detection and ranging”. It is a technique for optical distance measurements with laser pulses. Mounted on an airplane or helicopter, it is possible to create digital surface models. The product we use is also a point cloud. For every point, we also obtain

an intensity value. The big benefit of the LiDAR point cloud is that there is already some rough classification available. The colour of the points in *Figure 4* distinguishes between the height values. Both examples show the same scene.

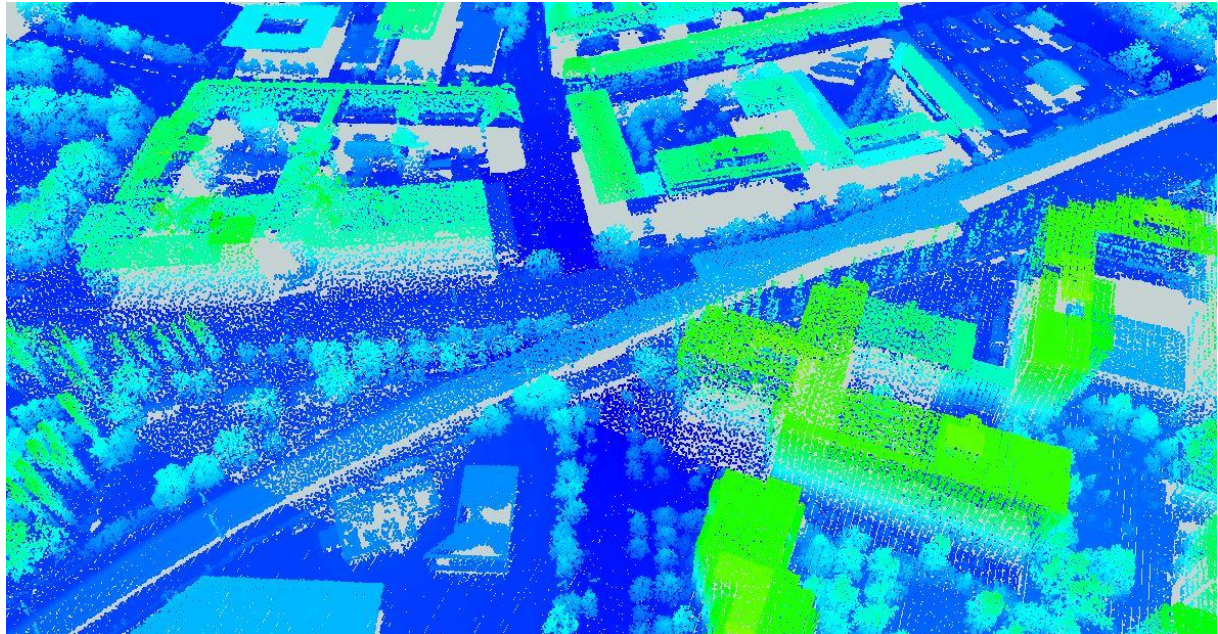


Figure 4, example of LiDAR dataset

3.4 FME

Feature Manipulation Engine (FME) is a tool developed by Safe Software. It is capable of visualizing and transforming lots of different kinds of data. The methods in FME are called transformers. In FME Workbench you can add readers for input files, place different transformers in order to manipulate your data and add writers to export the data into the file format you prefer. The FME Inspector allows visualizing data from files as well as intermediate products during the transformation process.



*Safe Software
(spatialbiz, 2020)*

FME is freely available for academic purposes and thus a good choice for us. There are many different transformers and the big community can help in a lot of difficulties that occur during the implementation.

4 Proposed workflow

4.1 Research questions

The main aim of our project was to enrich 2D road objects from ATKIS with information on the clearance space (relevant for underpasses and tunnels) derived from a point cloud.

Within a scope of this project we addressed several research questions:

- Is it possible to describe clearance space of bridges using LiDAR and bDOM data or fusion of those?
- Is it possible to extract relevant point cloud subsets depicting geometry of a bridge automatically using ATKIS data?
- Is it possible to create an automatic workflow to enrich the 2D ATKIS data with clearance space geometrical description?

4.2 Project architecture

4.2.1 General outline of the project

The general outline of a project assumed usage of 2D and 3D spatial information in order to assess clearance spaces of bridges and ultimately enrich 2D vector objects with estimated geometries (*see Figure 5*).

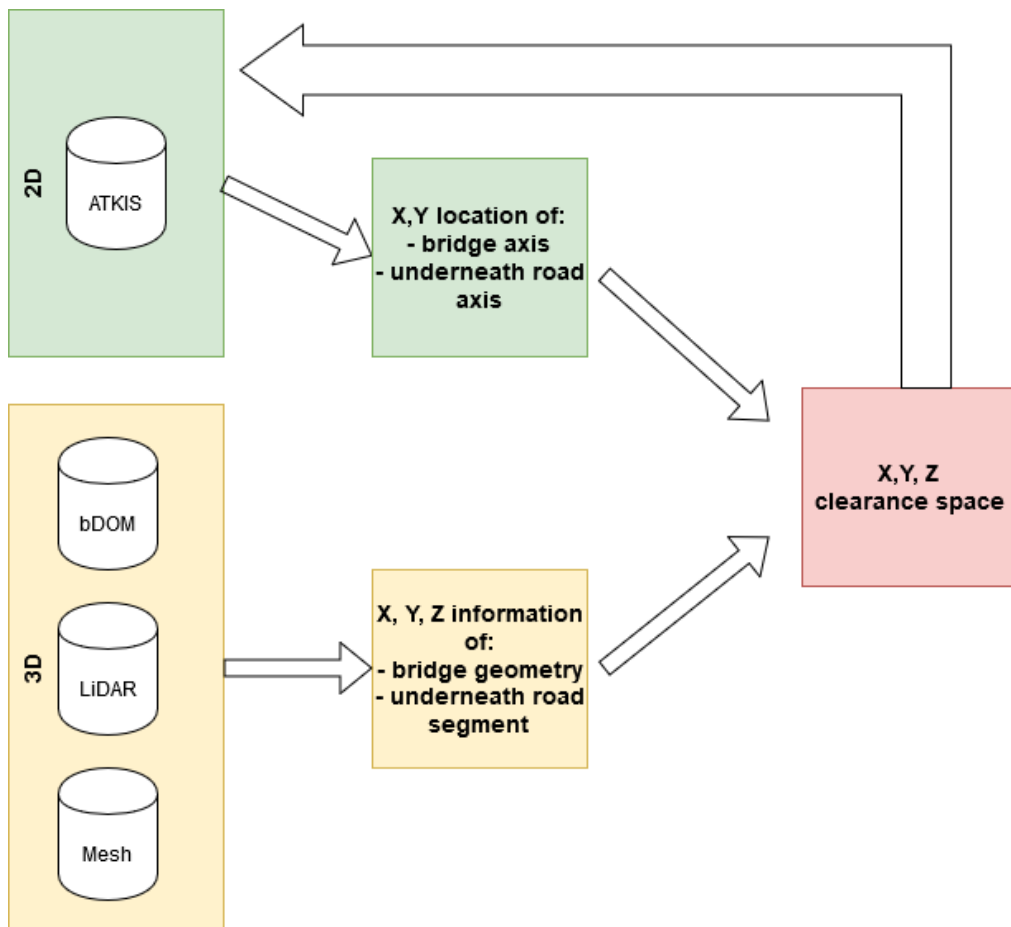


Figure 5, general workflow of the project

4.2.2 Detailed workflow of the project

As one of the research questions stated in the project was to determine which 3D spatial information source (bDOM, LiDAR or combination of those) could deliver the most accurate description of the clearance space it was essential to test a workflow with different scenarios of point cloud source. Mesh dataset was used only as a supportive 3D source to enhance visual inspection as it was already processed dataset.

First iteration and testing were conducted with only LiDAR point cloud as it presented the most promising results having classification attributes. One class was discarded at the beginning – nr 23 which, if exists, represents synthetically created ground surface i.e. below the bridge (Landesamt für Digitalisierung, 2016). The source of this synthetical creation is not known and could vary for different places (Landesamt für Digitalisierung, 2016) and also it is not present for all tested bridges. However, it could be considered for future research in clearance space assessment. Scenarios with different 3D datasets were also tested and a summary could be seen in chapter 6.1.19 The detailed approach outline could be seen in *Figure 6*.

We decided to test our solution for railroad bridges that intersect with the road axis. In ATKIS data there are different subsets representing the railroad axis (*ver03_1*) and road axis (*ver01_1*) as linear objects. Therefore, it was possible to narrow our field of searching for a bridge and intersecting road.

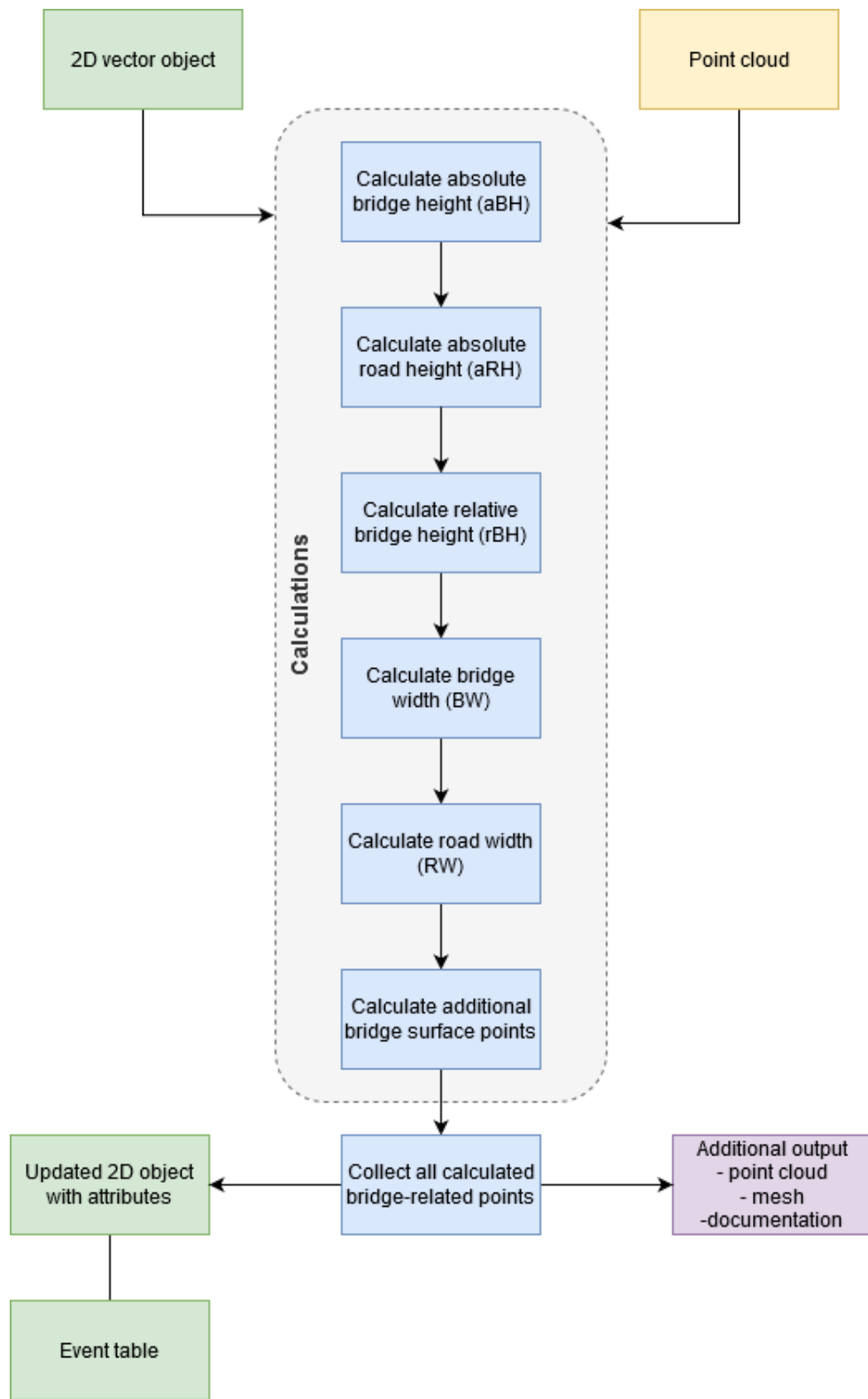


Figure 6, detailed workflow of the project

Each of the workflow steps (*blue boxes in Figure 6*) could be divided into substeps:

- **Calculate absolute bridge height**

ATKIS features have the attribute called *HDU_X (hatDirektUnten)*. This attribute describes the relation between overlying vector objects. (Geodäsie, 2010) (Fiutak, Marx, Willkomm, & Donaubauer, 2018) Attributes values are of type integer - e.g. value “0” means this feature does not overlay other features and “1” means this feature overlays one feature. Hence,

filtering segments by value equal 1 within the railroad axis subset has given locations of railroad bridges.

After the axis of a bridge of interest is selected, it is possible to buffer depending on a number of train tracks in the bridge segment which is possible to obtain from attribute GLS (*AnzahlDerStreckengleise*) (Geodäsie, 2010). Buffering distances are based on standard German gauge 1.435 m divided by 2 for one track railway and 2 m for two tracks (see *Table 1*). (Fiutak, Marx, Willkomm, & Donaubauer, 2018)

GLS value	Buffer distance [m]
1000	0.7175
2000	2

Table 1, bridge axis buffering based on GLS value

The calculated area represents not the entire span of a bridge but allows us to depict the core of a bridge segment.

Subsequently, this area was used to clip point cloud. Before that, the LiDAR dataset was filtered out by classes. LiDAR point cloud has an attribute “classification” which depicts several types of objects (Landesamt für Digitalisierung, 2016). The class which corresponds to bridge surface is either 20 (not in the documentation but confirmed by visual inspection that it depicts surfaces of bridges but also some high vegetation – but only if class 22 is not present) or 22 (only bridge surfaces). If there is class 22 present in a dataset there is no need to use class 20 and therefore it could be filtered out of further calculations. (Landesamt für Digitalisierung, 2016)

The final absolute bridge height (*aBH*) is calculated using the median value for a clipped point cloud.

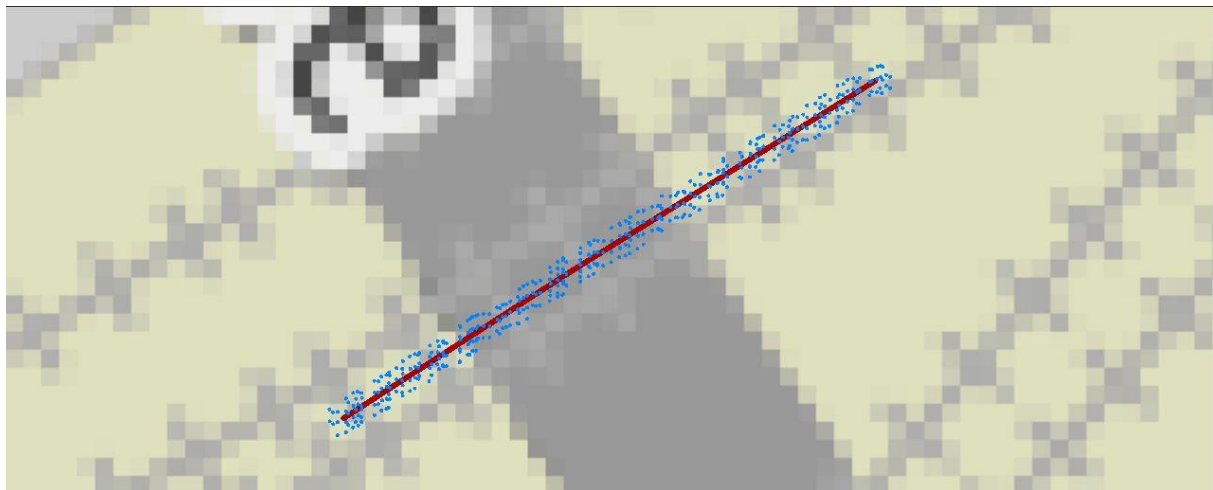


Figure 7, bridge axis (red line) and selected point cloud within buffered area (blue points)

- **Calculate absolute road height**

After the bridge of interest was selected it was possible to find corresponding underneath the road axis by finding intersecting road segment with a bridge segment. Then, point of intersection of two axis was created and buffered according to GLS attribute (see *Table 2*) of a bridge to get a rough estimation of bridge span and to surely cut road segment which is in the vicinity of the bridge but not too far to give bias for final absolute bridge height estimation. This step was made because the raw ATKIS road axis can be created by one relatively long segment and selection only by ID attribute will not be sufficient in each case.

GLS value	Buffer distance [m]
1000	10
2000	20

Table 2, road axis buffering based on GLS of corresponding bridge axis

To further narrow area of road height calculations the buffer around clipped road axis was made similarly like in aBH section. However, this time the attribute FSZ (*anzahlDerFahrstreifen*) was used. The value describes a number of lanes of a specific road segments. (Geodäsie, 2010) Lane width in Germany varies from 2.75 m to 3.75 m. (Bussgeldkatalog.net, 2020) Therefore, we decided to underestimate the width also taking into account that the road axis could not be accurately positioned in the centre of the road. The buffered values could be seen in *Table 3*.

FSZ value	Buffer distance [m]
[1-2]	1
[3-4]	1.5
[5-6]	2
[7 <	3
0 or missing	1

Table 3, buffering based on FSZ value

This allowed us to discard outliers and still extract the main sample of road height. The point cloud was filtered based on classification and only class of value 2 was selected which represents ground points.

The point cloud was clipped to the buffered area around road axis and the median value was used to determine absolute road height (aRH).

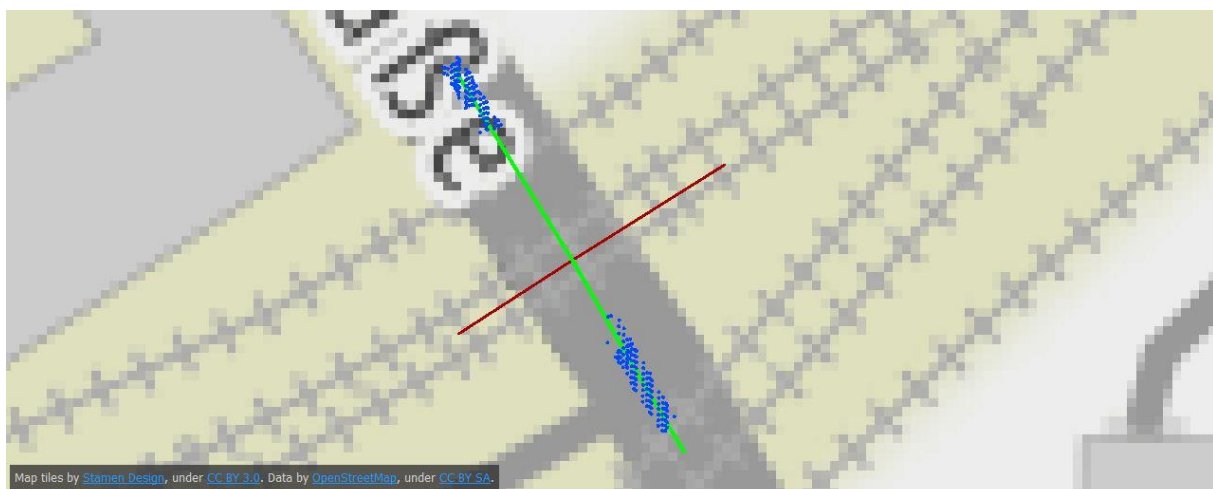


Figure 8, bridge axis (red line), corresponding road axis (green line) and selected point cloud within buffered road axis area (blue points)

- **Calculate relative bridge height**

To obtain the relative height of the bridge value aBH was subtracted from aRH giving final relative bridge height (rBH).

- **Calculate bridge width**

The selected road segment was draped on a point cloud which allowed to create a 3D line with a height position on every vertex. Raw ATKIS has a small number of vertices which do not allow to accurately drape a line on a point cloud. Therefore, vertices were densified in a way to interpolate correctly 3D line. The attribute which assesses those values is inherited from the bridge axis – GLS (see Table 4).

GLS value	Buffer distance [m]
1000	1
2000	2

Table 4, interval of vertex densification

This gives the opportunity to calculate a slope between each of vertices – highest values of slope percentage (>85%) describe parts depicting the end of bridge span - rest parts are filtered out.

```
@abs(((@Value(lastZ)-@Value(firstZ))/@Value(_length))*100)
```

Figure 9, formula to calculate slope percentage. “lastZ” stands for second in a row vertex of a line part, “firstZ” stands for first in a row vertex of a line part and “_length” is a line part length

Vertices creating lines are coerced to points. Mean value of X and Y position of those points creates maximum span position on each side of the bridge while min Z and max Z describe the maximum height of the bridge and minimum height on each side of the bridge respectively.

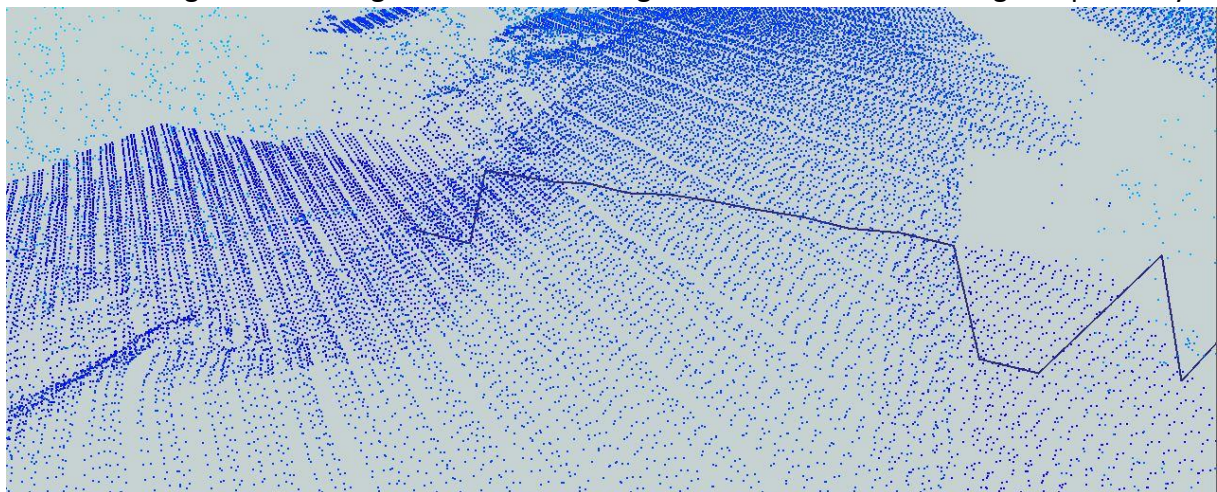


Figure 10, draped road axis on a point cloud

To prevent outliers the aBH attribute filters out highly or lowly elevated peaks with a threshold ± 1.5 m of aBH (Figure 10, peaks on the right).

Based on new points describing maximum height on each side of the bridge it was possible to connect them and calculate the length of this line which consequently measures the span of the bridge.

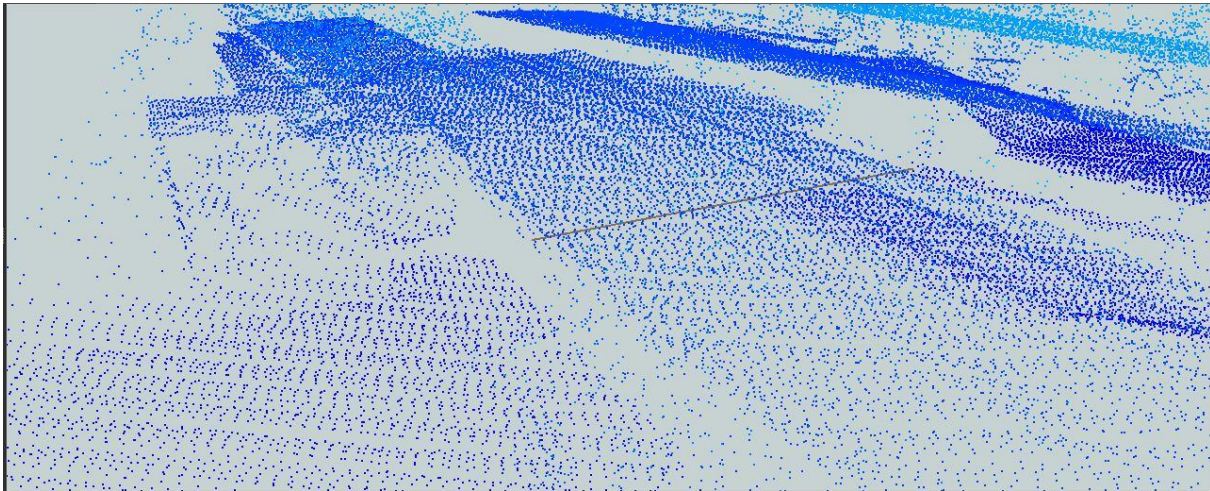


Figure 11, connected max height points describing width of the bridge

- **Calculate road width**

Based on ground points created in the previous step it was possible to localize cross sections on both sides of the bridge which were perpendicular to the road axis and at the same time projected to both edges of the bridge.

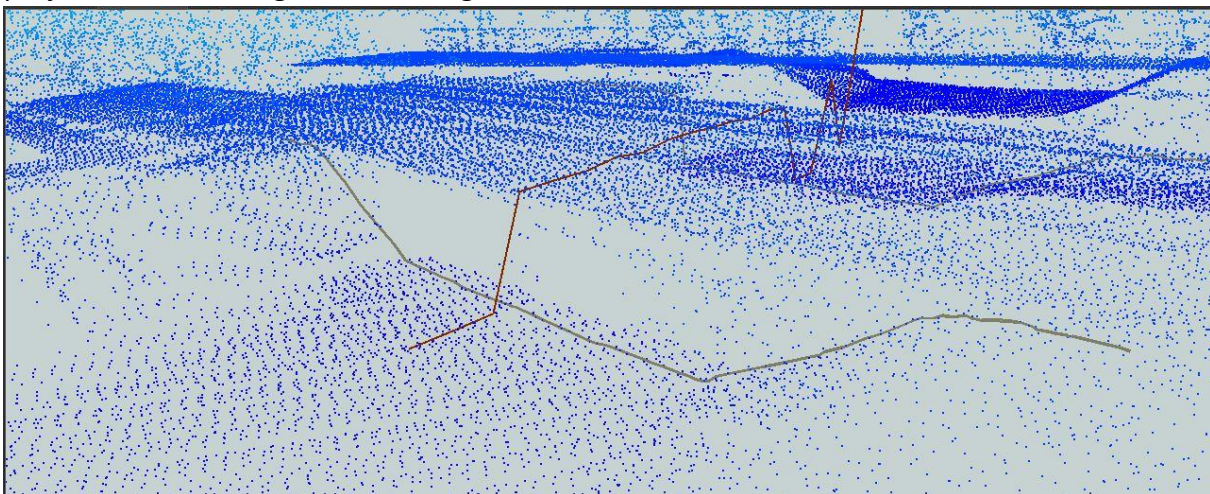


Figure 12, draped cross section (grey line) perpendicular to the road axis

These two cross-sections, one on each side of the bridge, are draped on the point cloud as seen in *Figure 12*. Every draped line gets chopped into points with an equidistance of 1 cm. Then for every point, the height difference to the 5th predecessor point as well as to the 5th successor point is calculated. If the absolute values of these height differences are within specific limits, the centres of mass of these points are selected as corner points where the road surface intersects with the bank. Combining the two corner points on each side of the bridge leads to the road width (*Figure 13, Figure 14*).

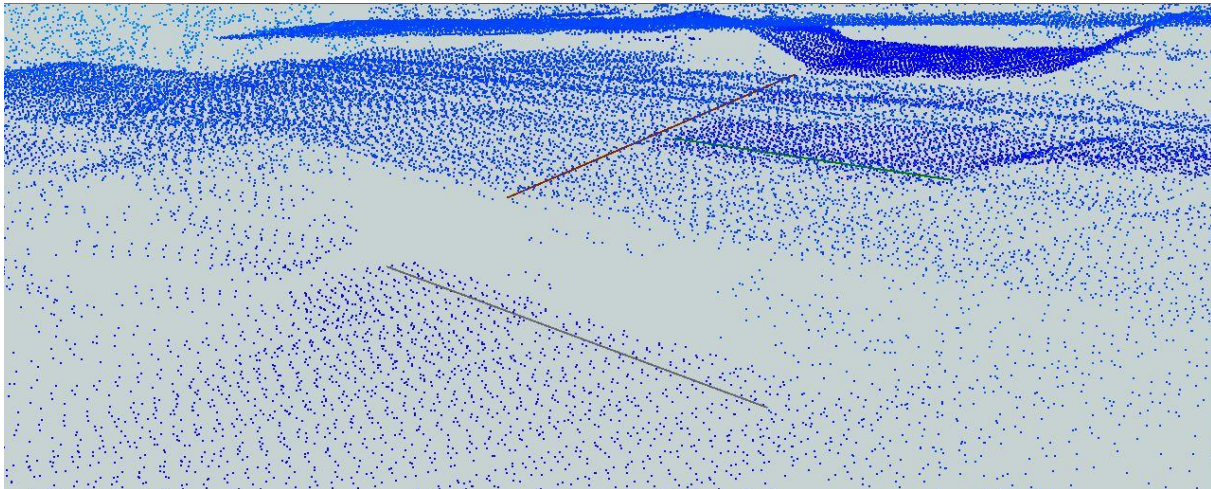


Figure 13, obtained road width directly underneath bridge edge (grey line)

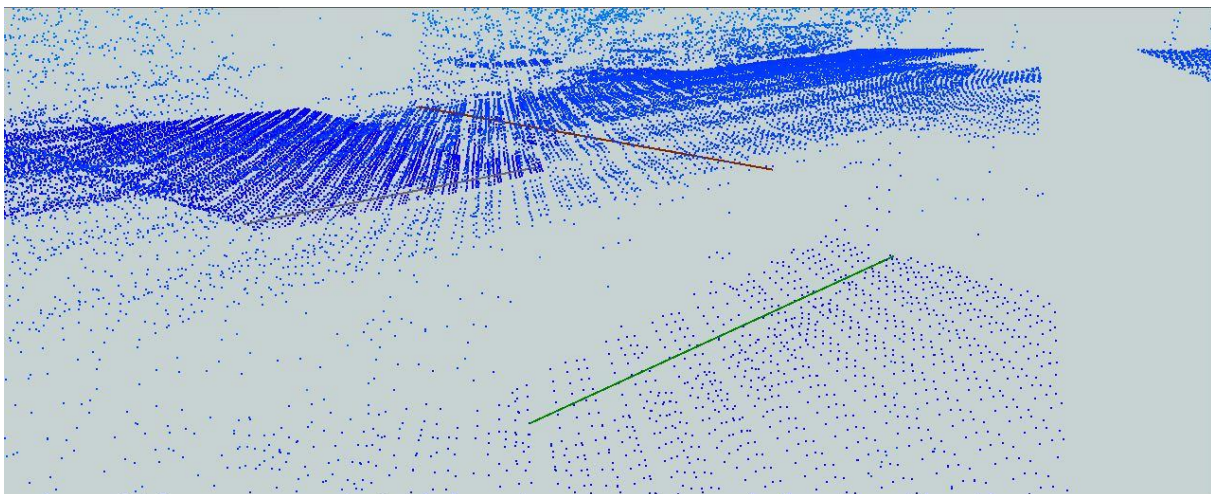


Figure 14, obtained road width directly underneath bridge edge, other side (green line)

- **Calculate additional bridge surface points**

To assess, additional corner points of the bridge the vertices creating bridge width were used. Each point on the ground was offset by rBH vertically. Thus, the rough position of top corner points was calculated. To obtain a more precise height coordinate, a 3D circular buffer with a 2 m radius was created in each top corner point. Then, the median height value was calculated and used to rectify the top corner position.

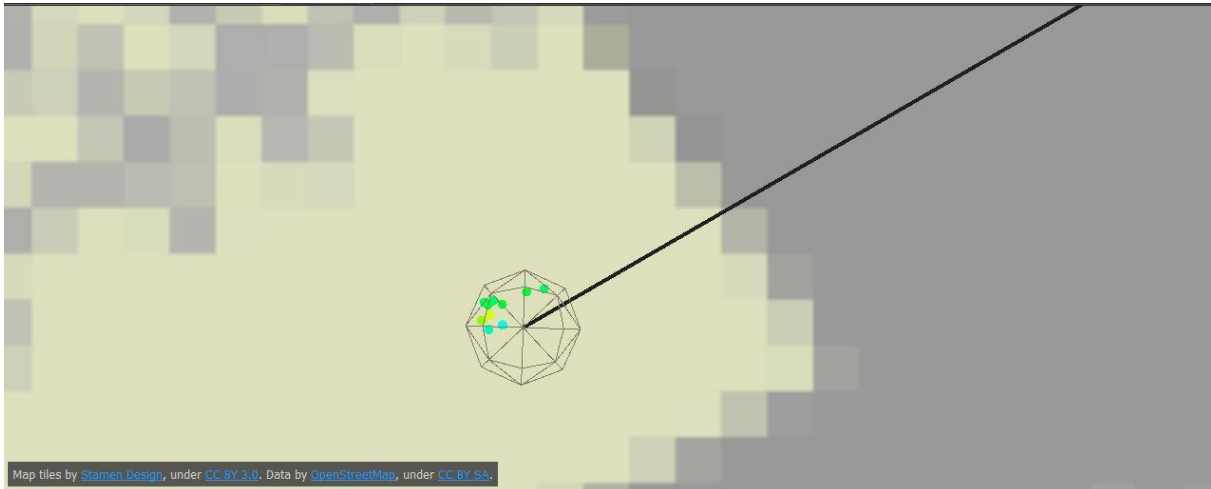


Figure 15, buffer around top corner point in 2D view. Point cloud within the buffer represented with multiple colours. Dark line represents bridge width

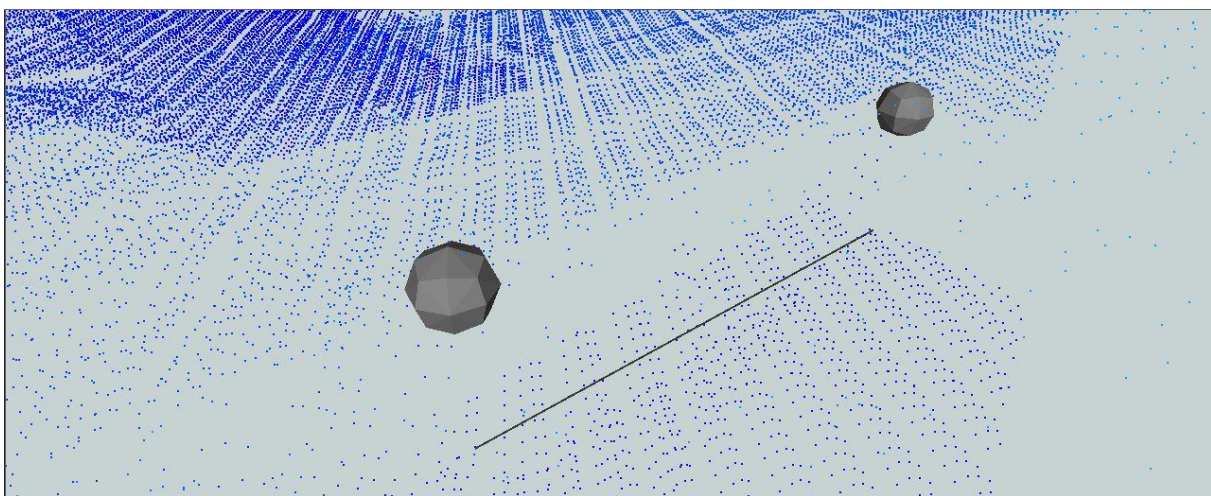


Figure 16, buffer around top corner point in 3D view (grey objects). Dark line represents bridge width



Figure 17, rectified positions of top corners (blue points). Grey line represents bridge width

- **Collect all calculated bridge-related points**

To all collected points, new attributes were assigned like unique ID and Foreign key creating a reference to specific bridge axis.

Moreover, as the calculated positions describing bridge clearance space were represented as points, we decided to use a Linear referencing system to save them in an event table. General attributes were saved to vector feature representing a bridge segment (see *Figure 18*).

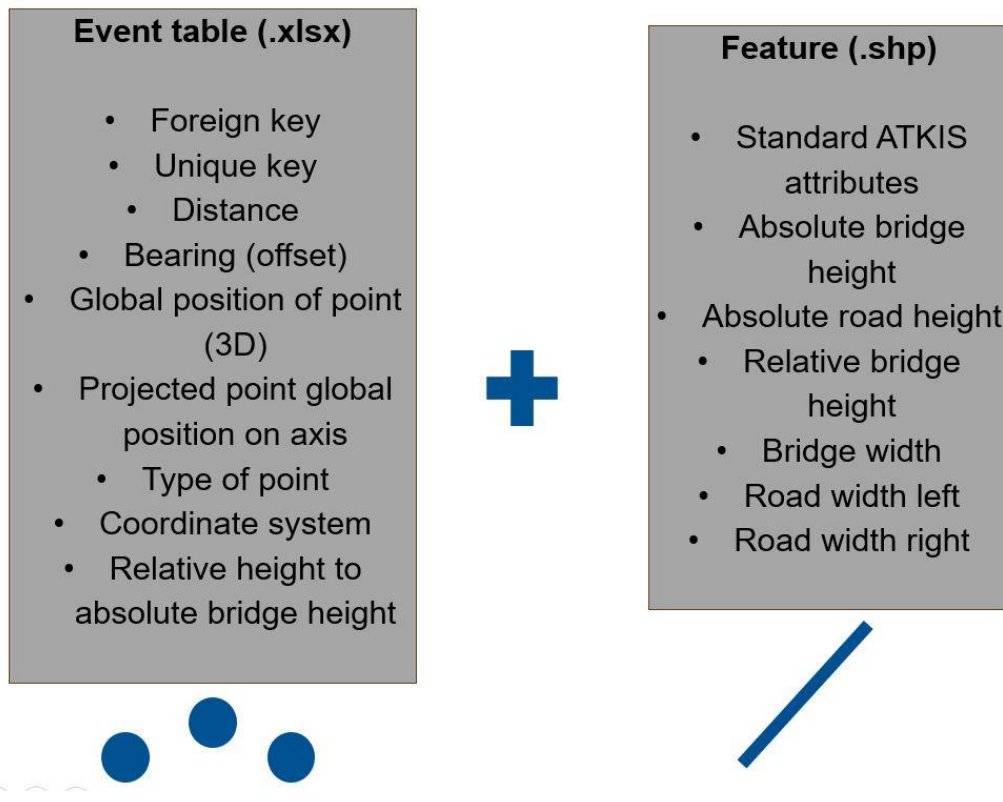


Figure 18, list of all collected and generated attributes

5 Study case areas

5.1 Bridge nr. 1 (urban area)

The first case study area is located near the railway station Munich East. This is already a complex scene because there are several bridges in close contact. In image nr. the line pointed in red depicts the axis of our railway bridge. The LiDAR point cloud from the northern view of the bridge is shown in *Figure 19*. The whole point cloud without a selection of a subset based on classification is visualized there. Obviously, we have many different objects in the scene like the bridge itself, banks, the road, pavements and lots of vegetation. The view to a picture (*Figure 21*) captured from the same direction shows, that there are more objects which were not directly visible in the point cloud-like barriers.

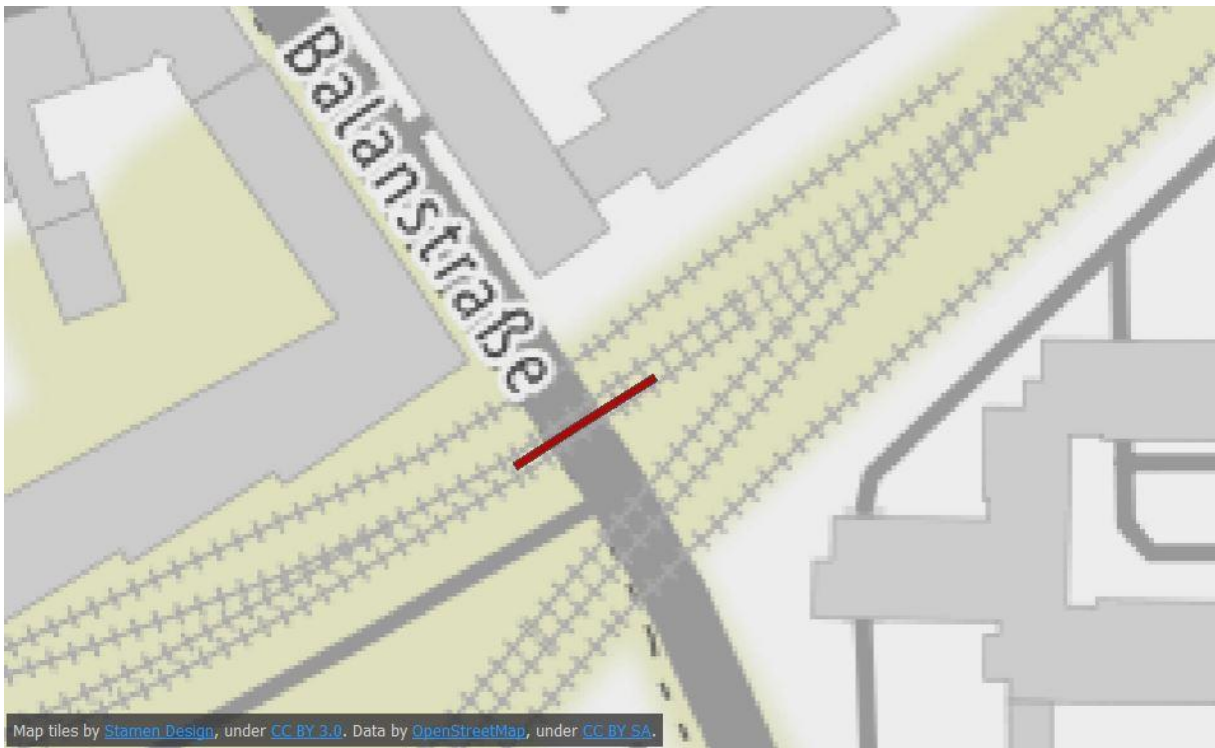


Figure 19, bridge nr. 1, ATKIS

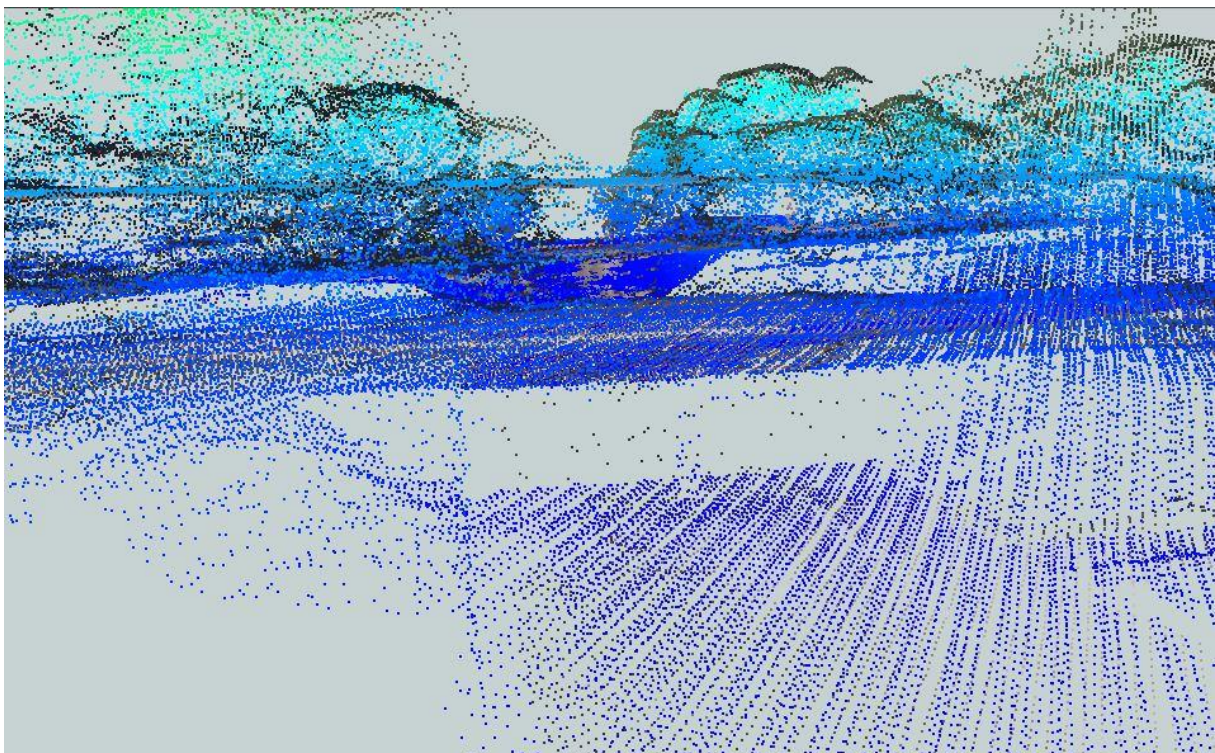


Figure 20, bridge nr. 1, LiDAR point cloud



Figure 21, bridge nr. 1, picture (Google, 2008)

5.2 Bridge nr. 2 (rural area)

The second bridge is located in the vicinity of Agatharied, a village south of Munich. As it is a rural area, there are fewer artificial objects than in the example before, but the vegetation is quite dense. *Figure 22* shows the digital orthophoto (DOP) of the bridge.



Figure 22, bridge nr. 2, DOP

5.3 Bridge nr. 3 (rural area)

This bridge is located in the vicinity of bridge nr. 2 and has similar framework conditions. The speciality about this bridge is, that there is a river located right next to the underneath road.

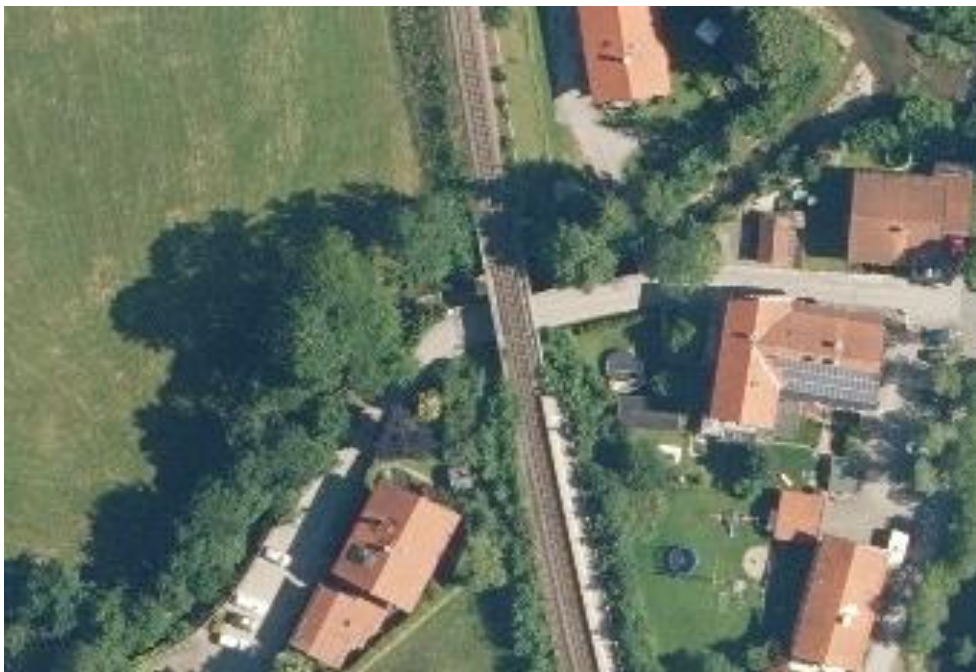


Figure 23, bridge nr. 3, DOP

6 Results

6.1 Clearance space creation with bDOM, LiDAR and fusion of those – comparison

Within the scope of the project, different sources of 3D spatial information were compared. As the most suitable source of information to assess clearance space of bridges was LiDAR. The main advantage of LiDAR is a classification attribute which allows to clearly separate point cloud depicting road and bridge surface. Therefore, vegetative objects are not inherited in the final assessment of the clearance space, which can be perceived as features giving the most bias to the final result.

Moreover, the LiDAR point cloud is denser than bDOM within city borders. This is not the case in a rural areas where bDOM has more points within an area of interest of a bridge core sample (described in 4.2.2). However, the bDOM point cloud could inherit vegetation and other not relevant objects within the core sample of a bridge which results in differences between absolute bridge height calculations (see *Table 5*).

As one of the solutions for the problem can serve a combination of LiDAR and bDOM point clouds. Nevertheless, bDOM still could give potential bias resulting from vegetation and other objects. Also, bDOM is convenient for the estimation of a bridge surface but not road height as it uses only class 2. Thus, relative bridge height and additional corner points could be falsely detected.

Example of bridge nr 1 shows that differences between bDOM and LiDAR are slight – were obstacles are not present. Therefore, we think that especially in rural areas we should depend on LiDAR as it is less likely to be biased by not relevant obstacles and the overall accuracy (like in bridge nr 1) is very similar.

Bridge nr	Number of points		Absolute bridge height [m]			bDOM vs. LiDAR [m]
	bDOM	LiDAR	bDOM	LiDAR	LiDAR + bDOM	
Bridge nr 1 (city)	263	451	530.80	530.81	530.80	-0.01
Bridge nr 2 (rural area)	183	60	721.53	721.34	721.49	0.19
Bridge nr 3 (rural area & river)	282	72	727.06	726.72	727.06	0.34

Table 5, comparison of bDOM and LiDAR for absolute bridge height estimation

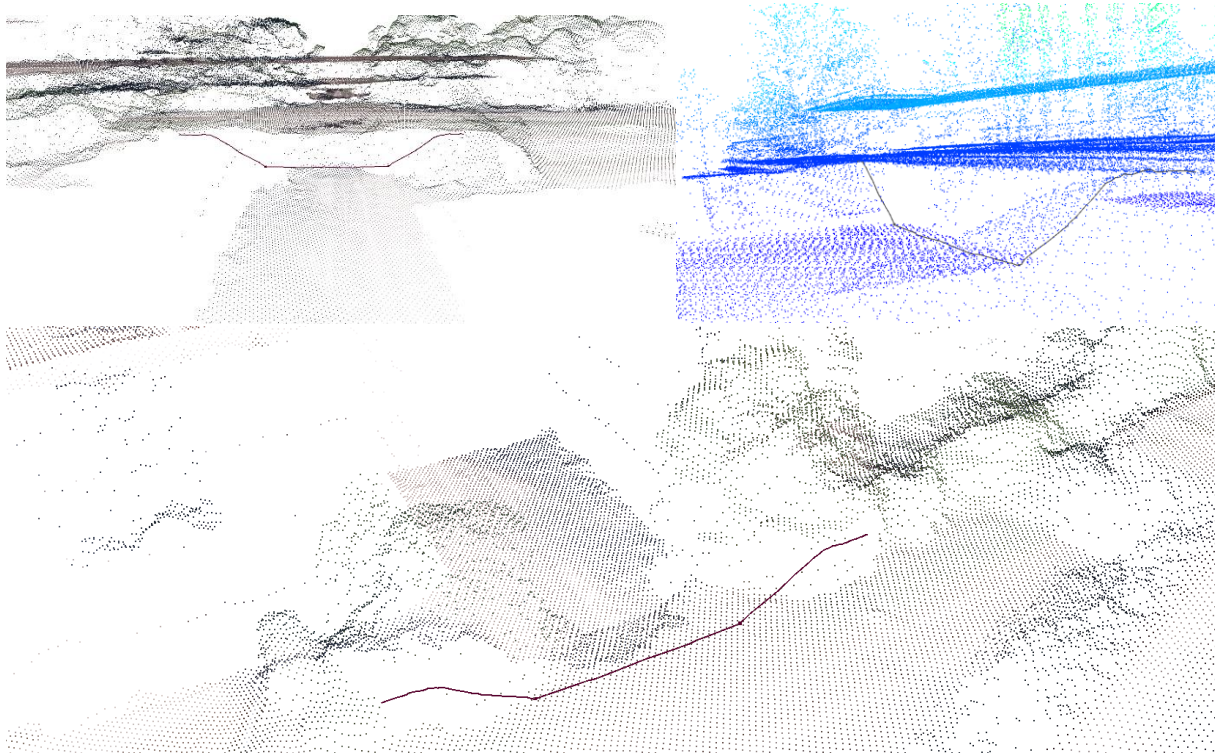


Figure 24, comparison of bDOM and LiDAR for road width estimation, bridge nr. 1

For our further analyses, we only used LiDAR point clouds because of the classification capabilities. The top right image in Figure 24 shows the vegetation above the banks of bridge 1. They have a light blue to green colour. It is remarkable that there exist some points underneath the dense vegetation at all. Unfortunately, the density here is not as high as on open areas. Based on these two facts, it is possible to extract the road width but only with an accuracy of ± 10 cm we would estimate. In the other two images, the draped cross section determined with LiDAR data is shown together with the bDOM point cloud. Due to the vegetation, there is not even one point in the dataset that would help to obtain the road width. This is another reason why we used LiDAR.

6.2 Extraction of point cloud subsets

As shown in section “proposed workflow” it is possible to clip out a specific bridge point cloud. Based on ATKIS attributes the bridge axes are selected and buffered to get a subset of points in the vicinity. Additional attributes of the ATKIS objects allow us to further specify the buffer distance for specific steps in the workflow.

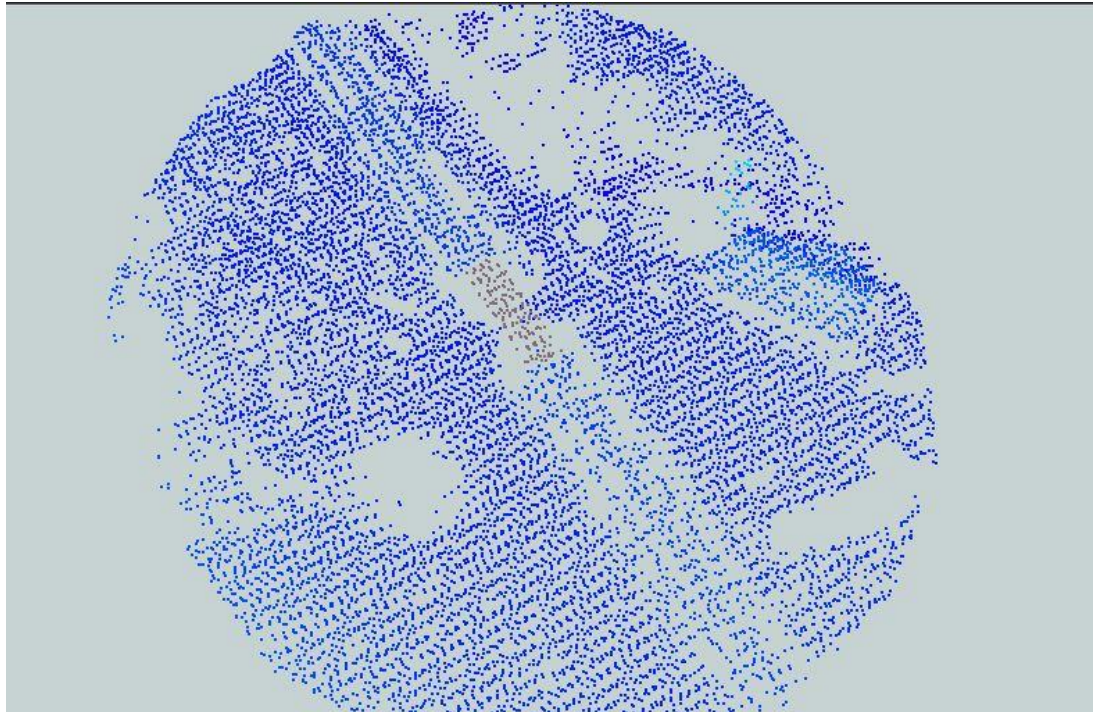


Figure 25, extracted bridge nr. 2 surface (brown colour) and its vicinity depicted by LiDAR point cloud

6.3 Linear referencing system (LRS)

The concept of LRS is an efficient way to handle data related to linear features. The attributes which are appropriate to a specific point are stored in a separate event table. This helps to keep the geometric data (the ATKIS shapefile) slim. To refer an event to a position, you need the foreign key of the object you are pointing to and two measure values, distance and bearing. The distance (measured along-track) contains the length from the starting point of the feature to the location of the event perpendicularly projected onto the linear feature. Bearing (measured across-track) is the perpendicular distance from the linear feature to the event.

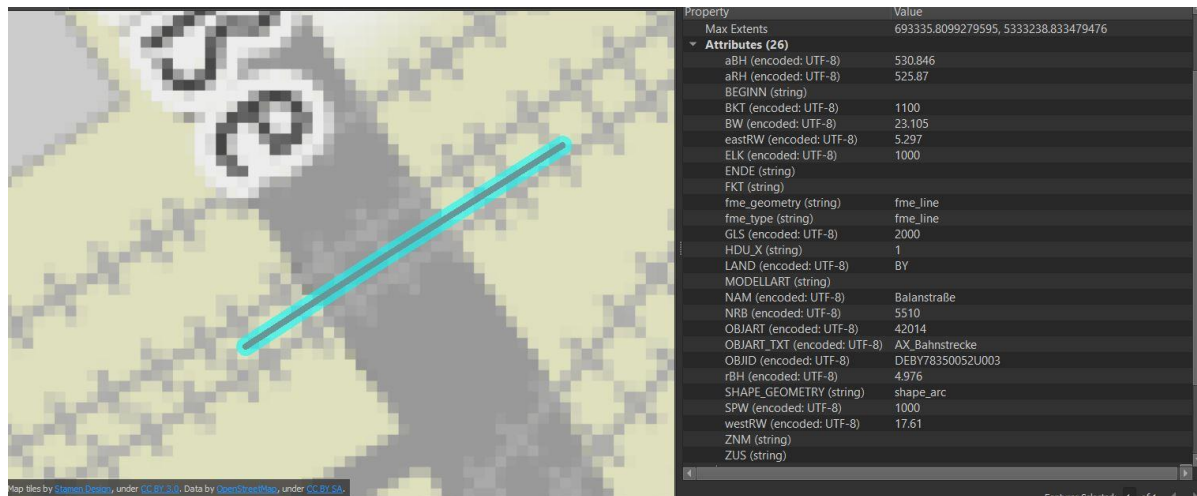


Figure 26, bridge nr. 1 as SHP file and additional attributes

	A	B	C	D	E	F	G	H
1	OBJID	ID	PType	S	OFFSET	PP_RH	PP_X	PP_Y
2	DEBY78350052U0C4eb5949f-1f36-443c-b2	PGround	6.247	-14.842	4.962		693309,4585	5333238,901
3	DEBY78350052U0C8fa95f97-c072-4493-83	PGround	11.543	-14.758	4.962		693313,86	5333241,848
4	DEBY78350052U0C08726507-0ad2-4df3-8	PSurface	11.996	-14.727	0.294		693314,3336	5333242,138
5	DEBY78350052U0Ce95ccce8-7a34-44f8-95	PGround	11.996	-14.725	5.013		693314,4178	5333242,192
6	DEBY78350052U0Cdfadf818-0ae1-4aea-6	PSurface	11.996	-14.725	0.314		693314,4178	5333242,192
7	DEBY78350052U0C2.404	PGround	2.404	-7.954	4.914		693319,2781	5333217,973
8	DEBY78350052U0C2.424	PSurface	2.424	7.955	0.093		693319,2951	5333217,983
9	DEBY78350052U0Cee7a90f5-63fc-439d-b'	PSurface	20.066	14.71	0.254		693321,1224	5333246,683
10	DEBY78350052U0C11.545	PGround	11.545	8.372	4.99		693327,0304	5333222,833
11	DEBY78350052U0C11.545	PSurface	11.545	8.372	0.076		693327,0304	5333222,833
12	DEBY78350052U0C20.112	PGround	20.112	8.726	4.965		693334,2391	5333227,262
13	DEBY78350052U0Cc7f999f8-6841-4867-99	PSurface	20.132	8.726	-0.033		693334,2561	5333227,272
14	DEBY78350052U0C20.132	PGround	20.132	8.726	0.03		693334,2561	5333227,272

Figure 27, part of the bridge nr. 1 event table

6.4 Automatic workflow to enrich ATKIS data

We managed to automate our workflow to a high degree, but it is not fully automatic. The only setting the user has to take is to select the designated bridge by its object ID. Then the whole workflow is done automatically. The calculated three-dimensional points are stored in an event table whereas some attributes are attached to the ATKIS shapefile. Additionally, a point cloud in different formats and a triangulated mesh grid as well as a documentation file (see Figure 29) with metadata to explain our abbreviations is processed.

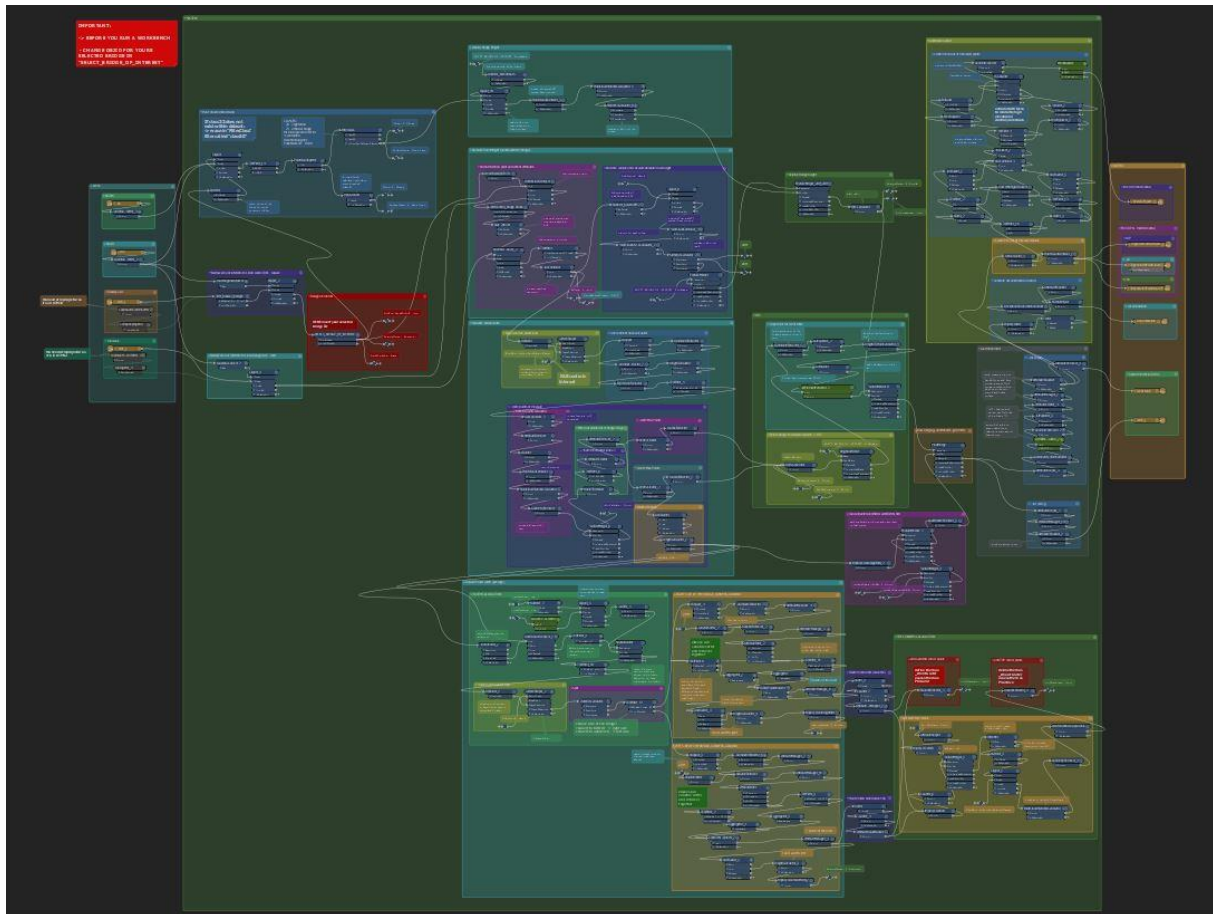


Figure 28, overview of FME Workbench – essential tool to prepare reproducible workflow

Attribute name	Attribute description
BW	Bridge width at the axis of the underneath road
CRS	Coordinate Reference System
ID	Unique ID
LX_0	X coordinate of starting bridge vertex
LY_0	Y coordinate of starting bridge vertex
OBJID	Foreign key (OBJID of bridge)
OFFSET	Distance from bridge to point. Negative number -> "Left side" is defined based on azimuth of the bridge measured counter-clockwise (West = 0 degrees) and points azimuth (West = 0 degrees). Left side points have larger azimuth than the bridge AND smaller azimuth than the bridge azimuth+180 degrees Positive number -> "Right side" is defined based on azimuth of the bridge measured counter-clockwise (West = 0 degrees) and points azimuth (West = 0 degrees). Right side is defined as opposite to the "Left side"
PL_X	X coordinate of measured point projected to line
PL_Y	Y coordinate of measured point projected to line
PP_RH	Relative height of point in reference to aBH (absolute bridge height)
PP_X	X coordinate of measured point
PP_Y	Y coordinate of measured point
PP_Z	Z coordinate of measured point
PType	Type of measured point (either representing ground or bridge structure)
S	Milage in meters starting in LX_0 and LY_0
aBH	Absolute bridge height
aRH	Absolute height of the road segment underneath the bridge
fme_dataset	D:\3_semestr\AppliedGeoinformaticsII\Test_2ndBridge\Agath aried\lidar_711_5294_all.las
fme_feature_type	ver03_1
fme_geometry	fme_undefined
fme_type	fme_no_geom
leftRW	Road width on the left side of the bridge. "Left side" is defined based on azimuth of the bridge measured counter-clockwise (West = 0 degrees) and points azimuth (West = 0 degrees). Left side points have larger azimuth than the bridge AND smaller azimuth than the bridge azimuth+180 degrees
rBH	Relative bridge height. Based on subtraction (aBH - aRH)
rightRW	Road width on the right side of the bridge. "Right side" is defined based on azimuth of the bridge measured counter-clockwise (West = 0 degrees) and points azimuth (West = 0 degrees). Right side is defined as opposite to the "Left side"

Figure 29, automatically generated documentation within FME Workbench

6.5 Point cloud as an additional modelling aid

Within scope of the project, additional outputs were delivered. One of those are point clouds generated out of measured points related to a bridge axis and saved in three different data formats (.xyz, .las, .csv). The created point cloud could serve as a modelling aid for designers and for visualisation purposes.

6.6 Mesh as an additional modelling aid

Besides the previously mentioned point cloud, we have developed the automatic generation of a mesh based on assessed clearance space positions. Thus, it is possible to present a clearance space as 3D objects. This feature of our workflow can help in the fast calculation of the clearance space volume and also aid visualisation.

6.7 Final results

For each study case bridge, we created reproducible results:

- ATKIS enriched shapefile (.shp)
- Event table (.xlsx)
- Point cloud (.xyz, .las, .csv)
- Mesh (.obj)
- Documentation (.docx)

6.7.1 Bridge nr. 1 (urban area)

The bridge located within a Munich city borders characteristics:

- High density point cloud available
- Class 22 not available, thus 20 was utilized
- Class 23 not available
- Low vegetation density
- 2 railway tracks present
- 1 feature underneath the bridge – road axis
- All automatic functions of workflow possible



A	B	C	D	E	F	G	H	I	J	K	L	M	N	O	P	Q	R	S	T
OBJID	ID	PType	S	OFFSET	PP_RH	PP_X	PP_Y	PP_Z	PL_X	PL_Y	LX_O	LY_O	CRS	aBH	aRH	rBH	BW	leftRW	rightRW
1	DEBY78350052U003	2a3f9fec-7731 PGround	2.39	7.95	4,91198443	693319,2696	5333217,967	525,9340156	693314,7412	5333224,51	693312,77	5333223,14	UTM32-WGS84	530.85	525.87	4.98	23.1	17.66	17.62
2	DEBY78350052U003	13a88aad-2a13 PSurface	2.41	7.05	0,093	693319,2866	5333217,978	530,753	693314,7577	5333224,52	693312,77	5333223,14	UTM32-WGS84	530.85	525.87	4.98	23.1	17.66	17.62
3	DEBY78350052U003	c29558a+1b1 PGround	11.54	8.37	4,99000848	693327,0304	5333222,833	525,8559913	693322,6368	5333229,72	693312,77	5333223,14	UTM32-WGS84	530.85	525.87	4.98	23.1	17.66	17.62
4	DEBY78350052U003	45b0ba6-841 PSurface	11.54	8.37	0,07647326	693327,0304	5333222,833	530,7695267	693322,6368	5333229,72	693312,77	5333223,14	UTM32-WGS84	530.85	525.87	4.98	23.1	17.66	17.62
5	DEBY78350052U003	3e4aed34-301 PGround	20.11	8.73	4,96509934	693334,2391	5333227,262	525,8809007	693329,3896	5333234,5	693312,77	5333223,14	UTM32-WGS84	530.85	525.87	4.98	23.1	17.66	17.62
6	DEBY78350052U003	68c394b9-36d1 PSurface	20.13	8.73	-0,033	693334,2561	5333227,272	530,879	693329,3861	5333234,51	693312,77	5333223,14	UTM32-WGS84	530.85	525.87	4.98	23.1	17.66	17.62
7	DEBY78350052U003	3be04656-b6d1 PSurface	20.13	8.73	0,03	693334,2561	5333227,272	530,816	693329,3861	5333234,51	693312,77	5333223,14	UTM32-WGS84	530.85	525.87	4.98	23.1	17.66	17.62
8	DEBY78350052U003	00ef412e-7d51 PSurface	20.07	-14.71	0,226	693321,1224	5333246,683	530,62	693329,3316	5333234,48	693312,77	5333223,14	UTM32-WGS84	530.85	525.87	4.98	23.1	17.66	17.62
9	DEBY78350052U003	788aff7a-9a99 PGround	20.05	-14.71	4,92714311	693321,1058	5333246,672	525,9188569	693329,315	5333234,47	693312,77	5333223,14	UTM32-WGS84	530.85	525.87	4.98	23.1	17.66	17.62
10	DEBY78350052U003	f8b10572-e4b0 PGround	12.0	-14.72	5,01325893	693314,4178	5333242,192	525,8327411	693322,6351	5333229,97	693312,77	5333223,14	UTM32-WGS84	530.85	525.87	4.98	23.1	17.66	17.62
11	DEBY78350052U003	b759ee62-0811 PSurface	12.0	-14.72	0,31405594	693314,4178	5333242,192	530,5319441	693322,6351	5333229,97	693312,77	5333223,14	UTM32-WGS84	530.85	525.87	4.98	23.1	17.66	17.62
12	DEBY78350052U003	2adbee36-bc11 PGround	2.59	-14.88	0,247	693306,4481	5333236,858	530,599	693314,9178	5333224,63	693312,77	5333223,14	UTM32-WGS84	530.85	525.87	4.98	23.1	17.66	17.62
13	DEBY78350052U003	56af1d3d-3bd1 PSurface	2.61	-14.88	0,247	693306,4481	5333236,858	525,9056787	693314,9013	5333224,62	693312,77	5333223,14	UTM32-WGS84	530.85	525.87	4.98	23.1	17.66	17.62
14	DEBY78350052U003	2adbee36-bc11 PGround	2.59	-14.88	4,88032131	693306,4314	5333236,847	525,9056787	693314,9013	5333224,62	693312,77	5333223,14	UTM32-WGS84	530.85	525.87	4.98	23.1	17.66	17.62

Figure 30, first bridge, updated ATKIS and event table presentation

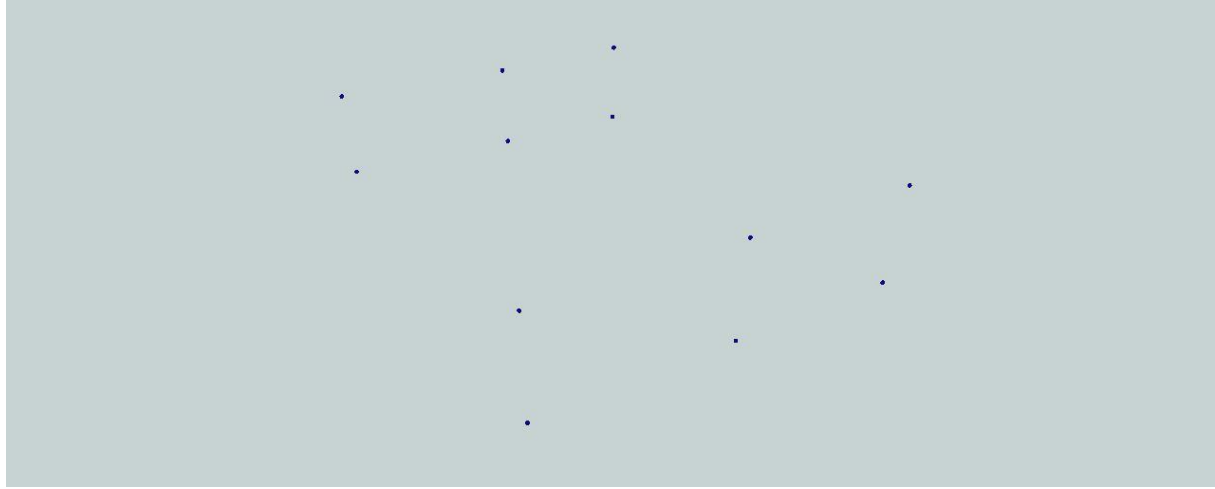


Figure 31, first bridge, generated point cloud

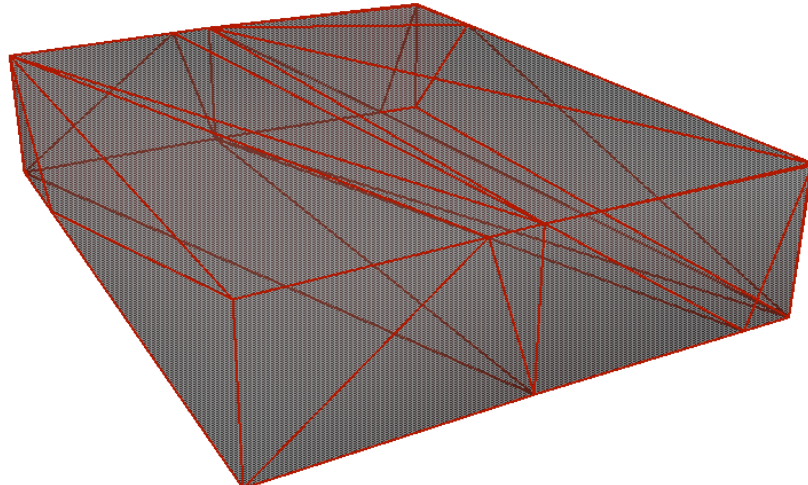


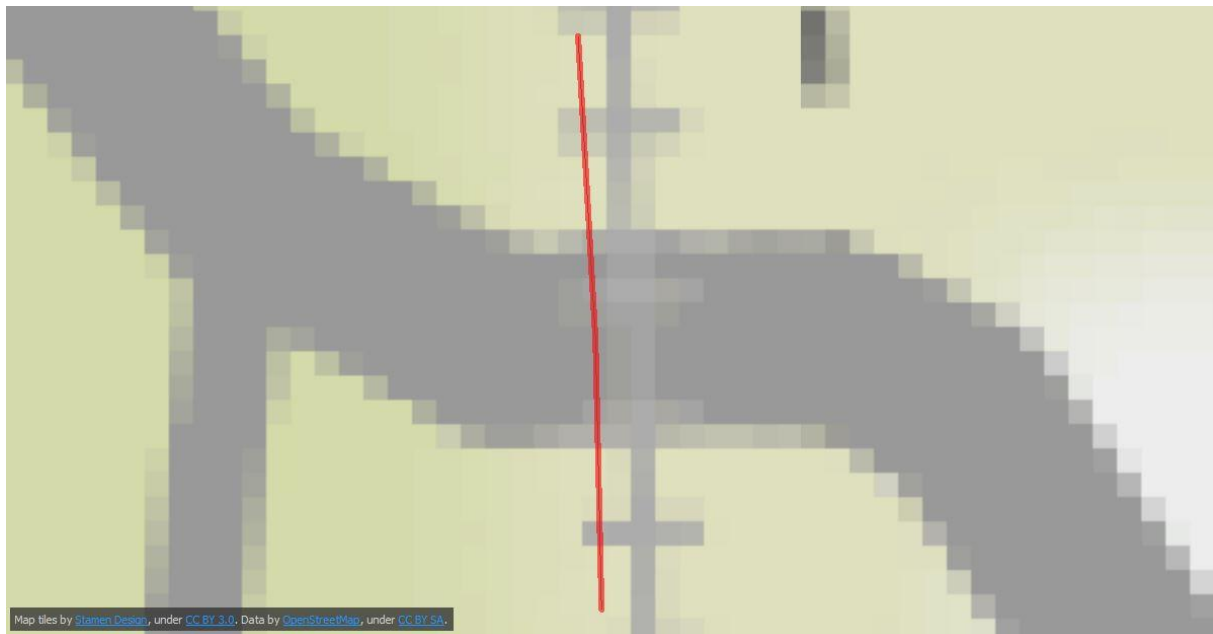
Figure 32, first bridge, generated mesh

6.7.2 Bridge nr. 2 (rural area)

The bridge located in south direction from Munich, near to village called Agatharied (in the vicinity of the bridge nr. 3), characteristics:

- Low density point cloud available
- Class 22 available, thus 20 was discarded
- Class 23 available but not used
- Medium vegetation density
- 1 railway tracks present
- 1 feature underneath the bridge – road axis

- All automatic functions of workflow possible



OBJID	ID	PType	S	OFFSET	PP_RH	PP_X	PP_Y	PP_Z	PL_X	PL_Y	LX
2	DEBYDLM0e50005P	f5321a9c-6678-4bd0-a533	PSurface	7.15	-2.327	-0.11	711585,2931	5294519,758	721,543	711582,9703	5294519,621
3	DEBYDLM0e50005P	6720c0be-16ab-4851-ac1	PGround	7.17	-2.329	3.955	711585,2939	5294519,778	717,4780901	711582,9692	5294519,641
4	DEBYDLM0e50005P	5d014bae-4c9b-48a1-9d1	PGround	8.646	-2.448	3.974	711585,3256	5294521,258	717,4589682	711582,882	5294521,114
5	DEBYDLM0e50005P	c9125d0a-0f68-4710-971	PSurface	8.646	-2.448	0.076	711585,3256	5294521,258	721,3570138	711582,882	5294521,114
6	DEBYDLM0e50005P	9b2371b9-1b0d-473d-8c	PSurface	9.635	-2.62	-0.08	711585,4065	5294522,346	721,513	711582,7978	5294522,1
7	DEBYDLM0e50005P	0581c1d0-3a70-4543-b1c1	PGround	9.655	-2.623	4.049	711585,4074	5294522,366	717,3840809	711582,7959	5294522,119
8	DEBYDLM0e50005P	3b8ef689-ac16-479a-918	PGround	9.933	2.861	3.994	711579,212	5294522,127	717,4393563	711582,7699	5294522,395
9	DEBYDLM0e50005P	4787862a-2e1f-4d42-a8c	PSurface	9.913	2.865	-0.075	711579,9193	5294522,107	721,508	711582,7717	5294522,376
10	DEBYDLM0e50005P	2050ddaa-afaf-4cc1-8dc1	PGround	9.462	2.903	3.984	711579,9243	5294521,054	717,4490464	711582,8141	5294521,927
11	DEBYDLM0e50005P	b80c2bf0-0e4f-4832-946	PSurface	9.462	2.903	-0.097	711579,9243	5294521,054	721,5304286	711582,8141	5294521,927
12	DEBYDLM0e50005P	78c5754b-adee-49be-94	PGround	7.215	3.309	3.929	711579,663	5294519,489	717,50424	711582,9665	5294519,685
13	DEBYDLM0e50005P	3e8a05b5-0f5-4b14-bc1	PSurface	7.195	3.312	-0.135	711579,6611	5294519,469	721,568	711582,9677	5294519,665

Figure 33, second bridge, updated ATKIS feature and event table presentation

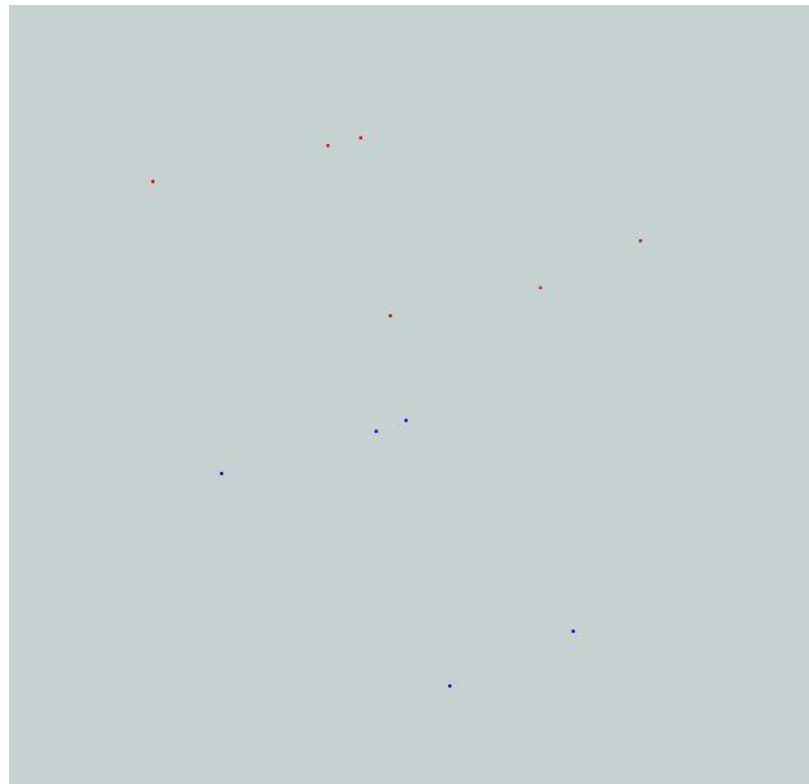


Figure 34, second bridge, generated point cloud

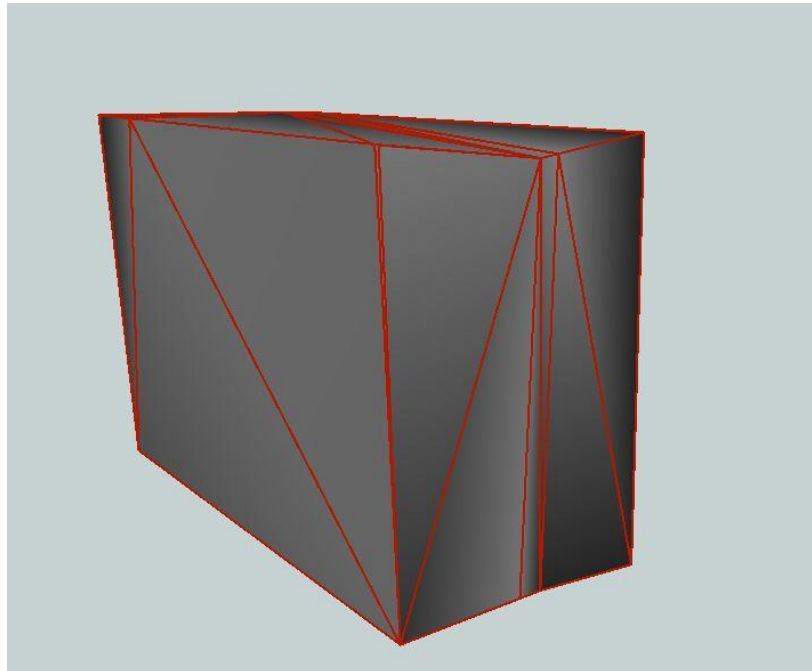
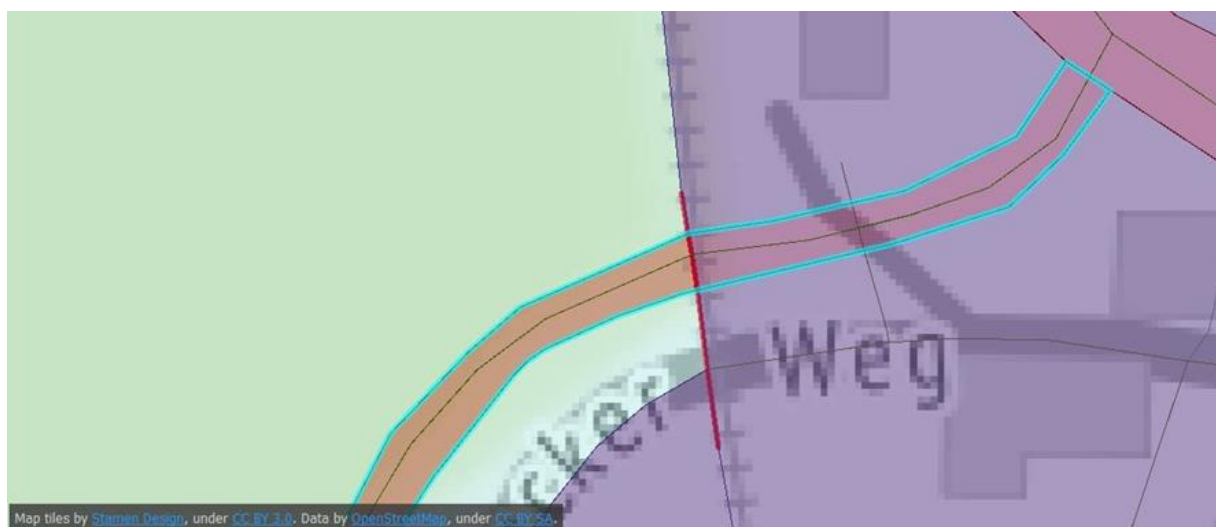


Figure 35, second bridge, generated mesh

6.7.3 Bridge nr 3. (rural area)

The bridge located in south direction from Munich, near to village called Agatharied (in the vicinity of bridge nr. 2), characteristics:

- Low density point cloud available
- Class 22 available, thus 20 was discarded
- Class 23 available but not used
- Medium vegetation density
- 1 railway tracks present
- 2 features underneath the bridge – road axis and riverbed
- All automatic functions of workflow possible



Map tiles by [Stamen Design](#), under [CC BY 3.0](#). Data by [OpenStreetMap](#), under [CC BY SA](#).

	A	B	C	D	E	F	G	H	I	J	K	L	
1	OBJID	ID	PType	S	OFFSET	PP_RH	PP_X	PP_Y	PP_Z	PL_X	PL_Y	PL_O	
2	DEBYBDLMeS0005y1zb3161c4-PGround	11.66	-1.91			4,630589682	711617,8266		5294203,125	722,3169103	711615,9404	5294202,82	711617,966
3	DEBYBDLMeS0005y1add8caaa-PSurface	11.64	-1.91			-0,0245	711617,8303		5294203,105	726,972	711615,9436	5294202,8	711617,966
4	DEBYBDLMeS0005y1ecedc538-PGround	9.22	-1.96			4,522150266	711618,2655		5294200,725	722,0253497	711616,3294	5294200,412	711617,966
5	DEBYBDLMeS0005y1da3c0fd-2PSurface	9.22	-1.96			-0,125119572	711618,2655		5294200,725	727,0726196	711616,3294	5294200,412	711617,966
6	DEBYBDLMeS0005y17043f09e-(PGround	6.65	-1.98			4,373948628	711618,7374		5294198,239	722,5735514	711616,7844	5294197,887	711617,966
7	DEBYBDLMeS0005y1b20a5001-PSurface	6.63	-1.98			-0,0845	711618,741		5294198,22	727,032	711616,788	5294197,867	711617,966
8	DEBYBDLMeS0005y1d9513a84-PSurface	6.78	2.42			-0,1645	711614,3797		5294197,584	727,112	711616,7615	5294198,014	711617,966
9	DEBYBDLMeS0005y124df1120-(PGround	6.8	2.43			4,463948982	711614,3691		5294197,601	722,483551	711616,7582	5294198,032	711617,966
10	DEBYBDLMeS0005y16ff286e2-1PGround	8.03	2.87			4,468104238	711613,7188		5294198,739	722,4793958	711616,5386	5294199,248	711617,966
11	DEBYBDLMeS0005y1b206b2b3-PSurface	8.03	2.87			-0,003791863	711613,7188		5294198,739	726,9512919	711616,5386	5294199,248	711617,966
12	DEBYBDLMeS0005y17381748-PSurface	10.89	4.11			0.0155	711612,0059		5294201,407	726,932	711616,0628	5294202,063	711617,966
13	DEBYBDLMeS0005y1bd54f3ab-(PGround	10.91	4.12			4,493222779	711611,9953		5294201,424	722,4542772	711616,0598	5294202,081	711617,966

Figure 36, third bridge updated ATKIS feature and event table presentation (highlighted riverbed in ATKIS dataset)

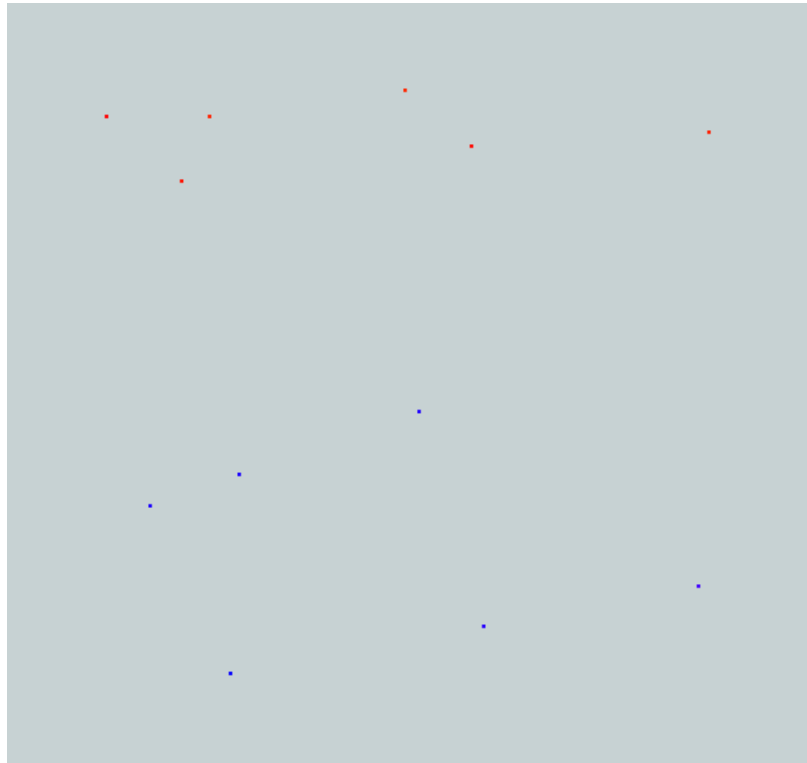


Figure 37, third bridge, generated point cloud

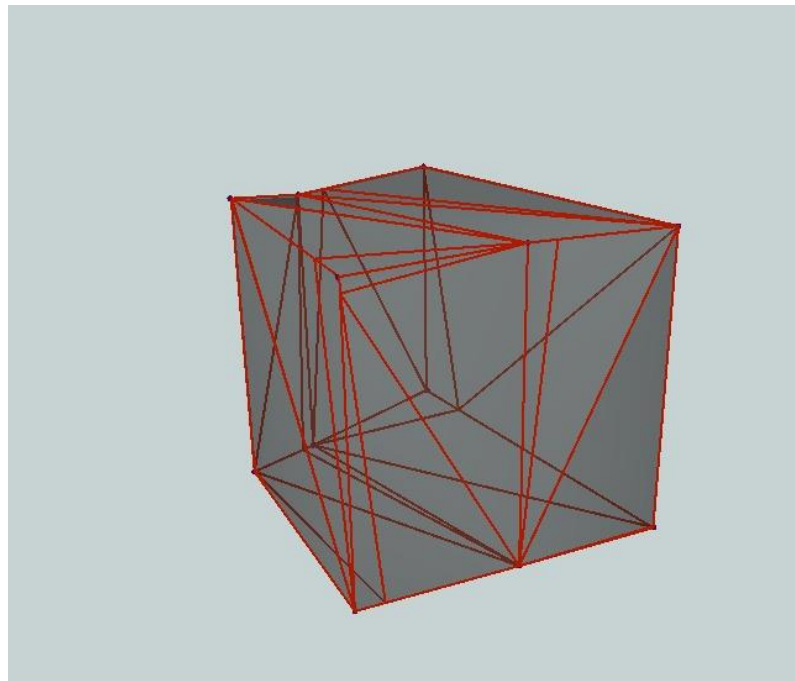


Figure 38, third bridge, generated mesh

7 Challenges

Although our method works well for different bridges and is generating reproducible results, it also has some limitations. The offset between the top bridge surface and the ceiling of the bridge remains undetectable. Even in the visual inspection of the point clouds, it is not possible to detect points on the edge of the bridge's ceiling. Some points which were found around that space cannot be certainly assigned either to the ceiling, a barrier or as an outlier.

Another challenge is the density of the point clouds. In the first study area, we have a high density where it is not a problem to extract additional points on the bridge surface, whereas the density for the other two bridges is much lower. Here it was problematic to extract enough points to calculate height.

We were also faced with varying classification categories in the LiDAR datasets. The class which corresponds to the bridge surface is either 20 or 22. According to our findings, when class 22 is present then this point cloud class should be used as it depicts only bridge surfaces (Landesamt für Digitalisierung, 2016). However, when class 22 is not present the class 20 should be used but it can inherit high vegetation beside bridge surfaces. Additionally, class 23 can serve as extra insight for clearance space reconstruction as it represents synthetically created ground surface i.e. below the bridge (Landesamt für Digitalisierung, 2016). However, this class is not always present and can vary in accuracy as the source of spatial information is not known (Landesamt für Digitalisierung, 2016). These points are arranged in a regular grid.

However, there could always be some exceptional cases. Not only a road passes bridge nr 3, but also a small river. It was difficult to implement an algorithm that extracts the road width for standard cases (bridge 1 and 2) and for this special case. In the end, it was also possible to solve this problem. We now have a method that is capable to analyse different bridge types. The result for bridge 3 is shown in Figure 39. The points on the lowest elevation (blue colour) represent the river.

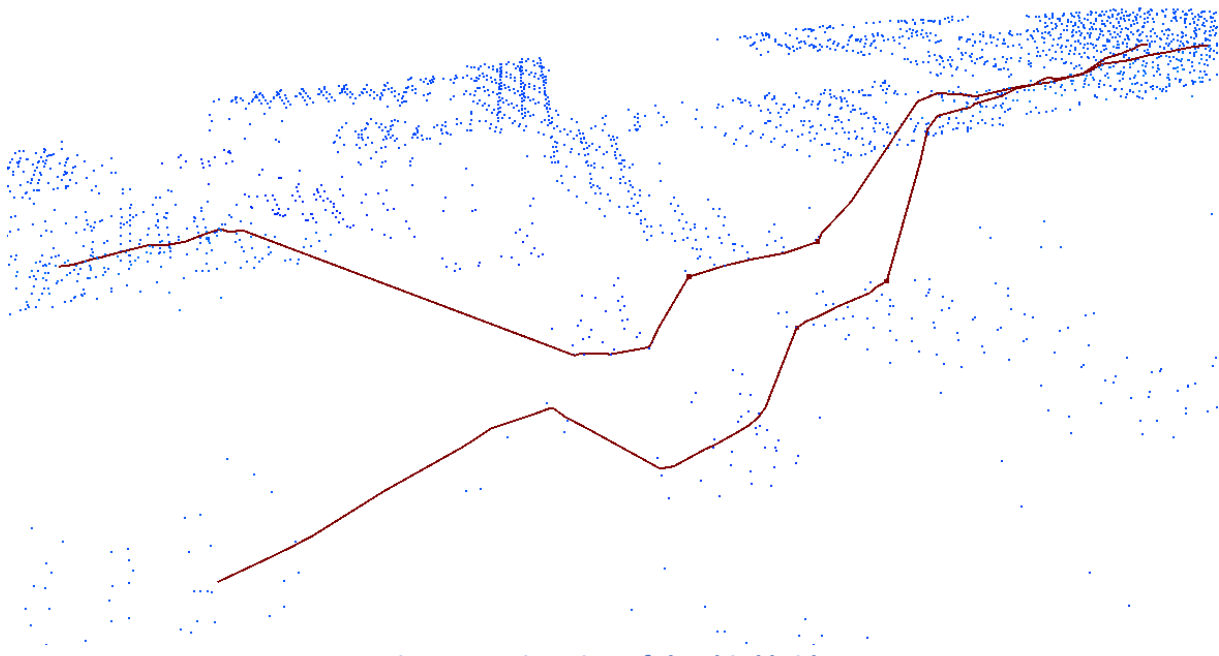


Figure 39, situation of the third bridge

Another problem is calculating the corner points of the bridge and the width of the road at the same time. As we can see in Figure 40, our approach is not exactly correct if the bridge and the underneath road intersect at an angle contrary of 90 degrees. Sometimes the ATKIS road axis is also not really parallel to the road borders or there is a curved section underneath the bridge as we have the example in bridge 3. The method is sufficient to determine the road width (intersection between road and banks) because we measure along perpendicular cross-sections. The only constraint is to select a cross-section that is not too close to the bridge to avoid intersections with the bridge. To determine the positions of the corner points (the intersecting points between road and bridge) one would have to construct a cross section parallel to the bridge axis to obtain a more sophisticated solution.

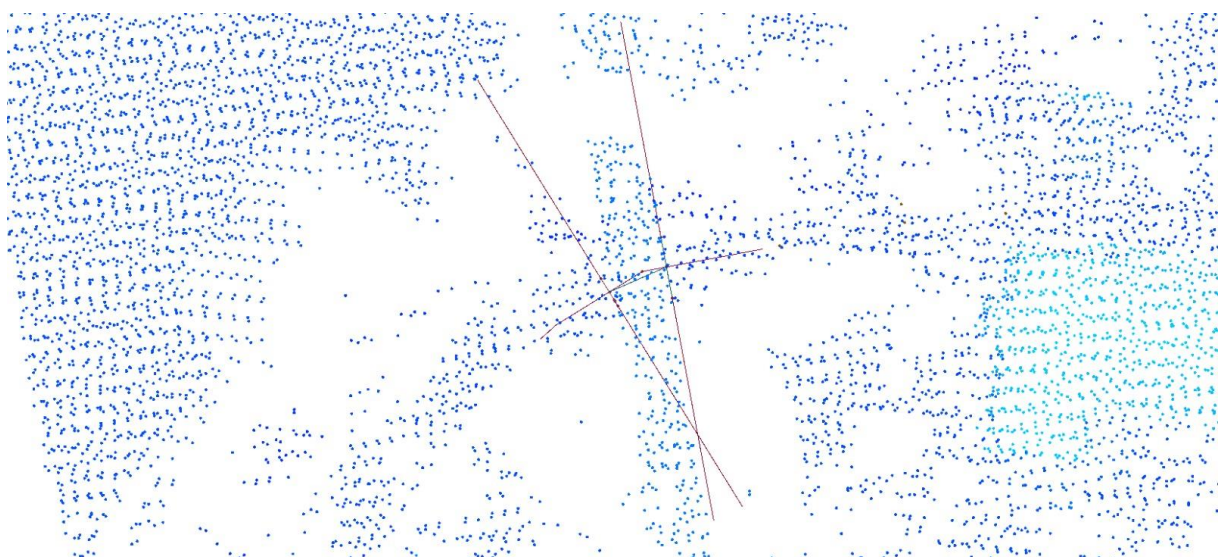


Figure 40, road axis curved at bridge 3

8 Summary and possible applications

Our task was to enrich the two-dimensional ATKIS data with information on the clearance space. In this project, we developed a workflow to automatically extract clearance information from point clouds using FME. We compared LiDAR and bDOM point clouds and preferred LiDAR in the end because of its classification. The result of our workflow is a simple geometric bridge profile consisting of 6 points for each bridge. Additionally, we attach some attributes like widths and heights to the ATKIS data. However, this approach also has some weaknesses which were mentioned already. We hope that our research can help to obtain a more sophisticated route planning under consideration of rough clearance heights at least.

Our findings do not solve ultimately the depiction of road clearance space. However, we believe that the solution can have already an application in manual clearance space modelling as it delivers rough geometrical shape of space underneath the bridge in widely used formats like *.obj (mesh)* or *.csv (point clouds)*. Moreover, detailed representations of road spaces can be utilized in areas like autonomous driving, driving simulators and emergency planning (Beil & Kolbe, 2017) (Schwab & Kolbe, 2019). The presented results can be also easily translated to standards like CityGML which can even further extend applications of our solution.

9 Bibliography

- Beil, C., & Kolbe, T. H. (2017). CityGML and the Streets of New York – A Proposal for detailed Street Space Modelling. ISPRS Annals of Photogrammetry, Remote Sensing and Spatial.
- Bussgeldkatalog.net. (2020). § 32 StVZO (*Abmessungen von Fahrzeugen u. Fahrzeugkombinationen*). Retrieved February 5, 2020, from <https://www.bussgeldkatalog.net/strassenverkehrszeitung/32-stvzo/>
- Cheng, L., Wu, Y., Wang, Y., Zhong, L., Chen, Y., & Li, M. (2015). *Threedimensional reconstruction of large multilayer interchange bridge using airborne lidar data*. IEEE Journal of Selected Topics in Applied Earth Observations and Remote Sensing, vol. 8, no. 2, pp. 691–708, Feb 2015.
- Consulting, N. 3. (2020, February 2). *Nektar 3D Consulting*. Retrieved from Nektar 3D Consulting Our Procedures: <https://nekta3d.com/consulting/our-procedures/>
- Donaubauer, A., Nguyen, S., & Gackstetter, D. (2019). *Applied Geoinformatics 2 Winter 2019/20*. München: Lehrstuhl für Geoinformatik, Technische Universität München.
- Elberink, S. O., & Vosselman, G. (2006). *3D MODELLING OF TOPOGRAPHIC OBJECTS BY FUSING 2D MAPS AND LIDAR DATA*. Proceedings of the ISPRS TC-IV Intl Symp on Geospatial Databases for Sustainable Development, Goa, India, pp. 17–30, 2006.
- Fiutak, G., Marx, C., Willkomm, P., & Donaubauer, A. (2018). *Projekt 3D Digitales Landschaftsmodell (3D-DLM) am Runden Tisch GIS e.V. - Abschlussbericht*. Runden Tisch GIS e.V.
- Gargoum, S., El-Basyouny, K., Gadowski, A., & Froese, K. (2017). *Automated Inventory of Overhead Assets on Highways using Mobile LiDAR Data*.
- Geodäsie, B. f. (2010). *Digitales Basis-Landschaftsmodell (AAA-Modellierung) Basis-DLM (AAA)*. Bundesrepublik Deutschland.
- Google. (2008, June). Balanstrasse 48. Munich, Bavaria, Germany.
- Ju, H. (2012). *A NEW APPROACH OF DIGITAL BRIDGE SURFACE MODEL GENERATION*. International Archives of the Photogrammetry, Remote Sensing and Spatial Information Sciences, Volume XXXIX.
- Landesamt für Digitalisierung, B. u. (2016). *Laserdaten Beschreibung der Punktklassen*.
- Liu, W., Chen, S.-e., & Hasuer, E. (2012). *Bridge clearance evaluation based on terrestrial lidar scan*. Journal of Performance of Constructed Facilities26 (4).
- Popescu, C., Täljsten, B., Blanksvärd, T., & Elfgrén, L. (2019). *3D reconstruction of existing concrete bridges using optical methods*. Structure and Infrastructure Engineering, V. 15.
- Puente, I., Akinci, B., González-Jorge, H., Díaz-Vilariño, L., & Arias, P. (2016). *A semi-automated method for extracting vertical clearance and cross sections in tunnels using mobile lidar data*. Tunnelling and Underground Space Technology59, 48-54.
- Schwab, B., & Kolbe, T. H. (2019). Requirement analysis of 3d road space models for automated driving. Singapore: ISPRS Annals of the Photogrammetry, Remote Sensing and Spatial Information Sciences.

- Sithole, G., & Vosselman, G. (2006). *Bridge detection in airborne laser scanner data*. ISPRS Journal of Photogrammetry and Remote Sensing, Vol. 61, Issue 1, pp. 33-46.
- spatialbiz. (2020). *FME Software*. Retrieved February 5, 2020, from spatialbiz: <https://www.spatialbiz.com/solutions/data-solutions/fme-software/>
- Vosselman, G., Elberink, S. O., Post, M., Stoter, J., & Xiong, B. (2015). *From Nationwide Point Clouds to Nationwide 3D Landscape Models*. Wichmann/VDE Verlag, Berlin & Offenbach, 2015.
- Wang, R., Peethambaran, J., & Chen, D. (2018). *LiDAR Point Clouds to 3D Urban Models: A Review*. IEEE Journal of Selected Topics in Applied Earth Observations and Remote Sensing.